JOURNAL OF GEOPHYSICAL RESEARCH, VOL. 102, NO. C8, PAGES 18,529-18,552, AUGUST 15, 1997

Effect of the overflows on the circulation in the subpolar North Atlantic: A regional model study

René Redler[1]
Institut für Meereskunde, Kiel, Germany

Claus W. Böning
Alfred-Wegener Institut für Polar- und Meeresforschung, Bremerhaven, Germany

Abstract. An ocean circulation model for process studies of the Subpolar North Atlantic is developed based on the Geophysical Fluid Dynamics Laboratory (GFDL) Modular Ocean Model (MOM) code. The basic model configuration is identical with that of the high-resolution model (with a grid size of 1/3° × 2/5°) of the World Ocean Circulation Experiment (WOCE) Community Modeling Effort (CME), except that the domain of integration is confined to the area from 43° to 65°N. Open boundary conditions are used for the inflows and outflows across the northern and southern boundaries. A comparison with the CME model covering the whole North Atlantic (from 15°S to 65°N) shows that the regional model, with inflow conditions at 43°N from a CME solution, is able to reproduce the CME results for the subpolar area. Thus the potential of a regional model lies in its use as an efficient tool for numerical experiments aiming at an identification of the key physical processes that determine the circulation and water mass transformations in the subpolar gyre. This study deals primarily with the representation and role of the overflow waters that enter the domain at the northern boundary. Sensitivity experiments show the effect of closed versus open boundaries, of different hydrographic conditions at inflow points, and of the representation of the narrow Faeroe Bank Channel. The representation of overflow processes in the Denmark Strait is the main controlling mechanism for the net transport of the deep boundary current along the Greenland continental slope and further downstream. Changes in the Faeroe Bank Channel throughflow conditions have a comparatively smaller effect on the deep transport in the western basin but strongly affect the water mass characteristics in the eastern North Atlantic. The deep water transport at Cape Farewell and further downstream is enhanced compared to the combined Denmark Strait and Iceland-Scotland overflows. This enhancement can be attributed to a barotropic recirculation in the Irminger Basin which is very sensitive to the outflow conditions in the Denmark Strait. The representation of both overflow regions determine the upper layer circulation in the Irminger and Iceland Basins, in particular the path of the North Atlantic Current.

1. Introduction

The Subpolar North Atlantic plays a key role in the circulation of the world's oceans as well as for the climate of northern Europe. Under present climate conditions the subpolar area represents the only source region for deep water in the northern hemisphere, associated with a vertical-meridional overturning circulation that imports relatively warm and saline surface waters from the south and releases large amounts of heat to the atmosphere in winter [*Schmitz*, 1995].

While of paramount importance for an understanding of North Atlantic climate variability, model simulations of the three-dimensional circulation in this area are much less advanced than simulations of the low- and midlatitude oceans. A prime reason is that the dynamics of the subarctic Atlantic is only weakly dependent on wind forcing and a linear vorticity balance (Sverdrup balance) is of little relevance [*Bryan et al.*, 1995]. Instead, the system appears to be controled by thermohaline factors like the heat and freshwater fluxes at the ocean surface, which are not known accurately,

[1]Now at Alfred-Wegener-Institut für Polar- und Meeresforschung, Bremerhaven, Germany.

Paper number 97JC00021.
0148-0227/97/97JC-00021$09.00

and small-scale processes like overflow and entrainment, which are difficult to implement in coarse-resolution circulation models. Due to the existing deficits in the modeling of this thermohaline system, our present quantitative understanding of the dynamics of the subpolar circulation is poor. The same holds for our knowledge concerning the dependence of numerical solutions on the representation of processes in models using different coordinate schemes, mesh sizes, and parameterizations.

Models of the large-scale ocean circulation have shown a rather wide spectrum of solutions for various aspects of circulation in the subarctic Atlantic. A particular area of difference concerns the horizontal structure of the subtropical gyre, manifested in the position of the subarctic front and the corresponding course of the North Atlantic Current (NAC). Earlier, "non-eddy-resolving" models often failed to simulate the observed northward current along the Grand Banks of Newfoundland. Instead of a subarctic front and eastward jet along 50° to 52°N, models typically generated a broad eastward flow between 40° and 45°N. A southward displacement of the frontal zone implied a strong error in the sea surface temperature over the Newfoundland Basin and, as shown by the heat budget analysis of a 2° × 2° model [*Sarmiento*, 1986], a strong, anomalous heat uptake by the ocean in the case of *Haney* [1971]-type heat flux conditions. Subsequent studies indicated that model simulations in this area are affected by numerical factors such as the choice of advection/diffusion schemes [*Gerdes et al.*, 1991] and by the horizontal resolution: a comparison of experiments carried out under the "Community Modeling Effort" (CME) of the World Ocean Circulation Experiment (WOCE) showed that a fine grid (1/3° × 2/5°) resulted in a more realistic position of the subarctic front in the Newfoundland Basin (i.e., near 50°N) than a non-eddy resolving grid (with 1° × 1°) [*Böning et al.*, 1996]. A still unsatisfactory feature of the high-resolution CME model was, however, the course of the NAC farther downstream where the bulk of the flow turns northward west of the Mid-Atlantic Ridge (MAR) (Figure 1). The behavior has been attributed to the artificial, closed boundary at 65°N in that model which prohibits an outflow of surface water into the Norwegian Sea. It stands in contrast, however, to the flow field in other models with a similar northern boundary but a NAC that crosses the MAR south of 52°N, e.g. the world ocean model (1/2° × 1/2°) of *Semtner and Chervin* [1992]. It is one of the objectives of the present study to shed some light on the model factors that affect the NAC in the northeastern North Atlantic.

A fundamental discrepancy between different large-scale circulation models concerns the sources of North Atlantic Deep Water (NADW) and the dynamical response of the meridional overturning to anomalies in the atmospheric forcing. Many coarse-resolution models of the thermohaline circulation exhibit a strong sensitivity of the deep water renewal rate to the surface fluxes of heat and fresh water over the subarctic Atlantic, south of the Greenland-Scotland Ridge [*MaierReimer et al.*, 1993; *England*, 1993]. Changes in the convective activity, e.g., by freshwater anomalies over the Labrador Sea, lead to changes in the meridional overturning circulation [*Weisse et al.*, 1994]. A corresponding behavior is manifested in the interdecadal oscillations in North Atlantic climate found in an coupled ocean-atmosphere model [*Delworth et al.*, 1993]: the intensity of the thermohaline circulation appears intimately related to density anomalies over the western portion of the subpolar gyre. A strikingly different behavior was found in a series of CME experiments. The production of 2000-m-deep columns of homogenized water by convective mix-

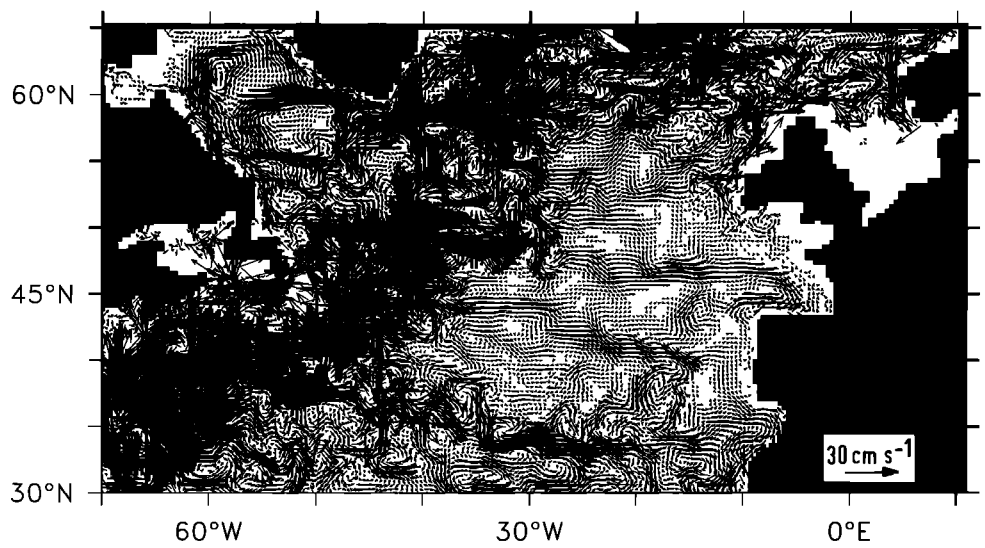

Figure 1. Snapshot of the horizontal velocity in centimeters per second at level 5 (175 m) for CME experiment K13-4.

ing in the central Labrador Sea had a negligible effect on the net production and outflow of deep water [*Böning et al.*, 1996]. Instead, the overturning was essentially controlled by the conditions in the overflow regime, in the CME given by a damping toward specified hydrographic conditions adjacent to the closed boundary at 65°N. Anomalies in the surface fluxes over the subpolar basin south of 65°N, even if leading to a complete shutdown of deep winter convection, had a negligible effect on the transport as long as there was a source of dense overflow water near the northern boundary [*Döscher and Redler*, 1997].

A critical factor controlling the behavior of numerical models in the subarctic Atlantic therefore seems to be the representation of the outflows of dense water from the Nordic Seas, constituting the densest contribution to NADW. From observations it has been estimated that about 2.9 Sv are spilled out through Denmark Strait [*Ross*, 1984], 1.9 Sv through the Faeroe Bank Channel [*Saunders*, 1990], and about 1 Sv across some notches in the Iceland Faeroe Ridge [*Meincke*, 1983]. The fast, bottom-intensified outflows are believed to entrain ambient water as they plunge south of the sills and merge with other deep water masses recirculating in the Irminger and Iceland Basins, i.e., Labrador Sea Water (LSW) and the remnants of Antarctic Bottom Water [*McCartney*, 1992]. This leads to some modification of the original water mass signature and a roughly twofold increase of transport [*Dickson and Brown*, 1994; *Price and Baringer*, 1994]. The small-scale nature of both the overflow process itself and of the entrainment of ambient water south of the sills essentially prohibits an explicit simulation of these processes in coarse-resolution circulation models; their net effect on the production rate and the density of NADW becomes dependent on a number of numerical factors: coordinate schemes, discretization of topography, and mixing parameterization.

Attempts to capture this net effect of the outflows basically follow two different lines. One is to explicitly include the exchange of water between the Nordic Seas and the Atlantic proper. Apart from the difficulty of realistically simulating the water mass conversions in the Greenland and Norwegian Seas, models that do not resolve the small-scale Rossby radii (of the order of 10 km) over the Greenland-Scotland Ridge cannot generate shears sufficient to break the rotational constraint that causes the deep flow field to be guided by the topographic contours. Deep flows across a steep ridge in that case become mainly dependent on friction [*Gerdes*, 1993b]; usually transports are very weak unless the ridge topography is artificially modified (deepened) [*Roberts and Wood*, 1997]. This problem may, to a certain extent, be alleviated in the present generation of eddy-resolving models with grid sizes of 10 to 15 km being run by several groups in Europe and the United States that begin to resolve important topographic features like the Faeroe Bank Channel. A potentially serious error of models formulated in a geopotential or z level coordinate system is their inability to simulate the downslope advection of dense water, without artificially inducing strong diapycnic mixing (by the standard convective adjustment schemes) and hence blurring of the water mass signature. Alternatives offered to alleviate this problem are the use of bottom boundary layer formations based on terrain-following (σ) coordinates [*Beckmann and Döscher*, 1997] or of models formulated in isopycnic rather than z coordinates. The effect of different coordinate schemes in models of medium-resolution has been discussed by *Gerdes et al.* [1991], *Roberts et al.* [1996], and *Chassignet et al.* [1996]. A rigorous intercomparison of high-resolution models based on different coordinate schemes, and their respective parameter dependencies, is not available yet.

An alternative approach adopted in ocean-only models not aiming at a simulation of the exchange with the Nordic Seas itself has been to abandon an explicit modeling of the overflow and to incorporate their effect diagnostically. In Atlantic models like that of *Sarmiento* [1986] and the CME [*Bryan and Holland*, 1989] the simulated temperatures and salinities adjacent to the closed northern boundary are damped toward observed values in order to incorporate the effect of the water mass transformation taking place in the Nordic Seas. While with this approach it seems possible to capture the effect of the outflow on the basin-wide overturning [*Döscher and Redler*, 1997], there are certain problems with respect to the regional circulation structure in the northeastern North Atlantic. First, the presence of Iceland prevents a zonal redistribution of water within a narrow buffer zone adjacent to a boundary at 65°N, leading to deficits in the horizontal structure of the flow field, for example, the course of the NAC. Second, a zonal wall chosen according to the latitude of the Denmark Strait lies north of the Iceland-Scotland Ridge, rendering its overflow still subject to explicit modeling.

The host of model problems and dependencies outlined above, concerning the simulation of an ocean area of key importance for climate and climate variability, clearly calls for a better understanding of the model factors that affect the circulation and water mass distribution in the Subpolar North Atlantic. Attempts to rationalize differences in model behavior such as those outlined above are hampered by the fact that the underlying model configurations differ in more than one respect. Because of the number of poorly known model aspects and parameters involved in that problem, combined with the need for a grid size sufficiently small to resolve, at least marginally, the boundary currents and frontal structures in the area, a systematic investigation cannot involve the whole North Atlantic but has to be restricted regionally. As a suitable southern limit for studies of the subpolar gyre dynamics we propose the latitude 43°N which intersects the western boundary near the southern tip of the Grand Banks. The model basin thus excludes the Gulf Stream regime but includes the NAC with the associated subartic front. In-

flows and outflows across the southern boundary, which at that latitude are mainly taking place in the western boundary current regime, have to be modeled by open boundary conditions. In this study we present a subpolar model developed from the CME configuration, with an identical horizontal grid and the same location of the northern boundary. This provides us with a basis to test the behavior of the regional model against a full Atlantic model and with a baseline of existing sensitivity studies to build on. The first set of experiments, presented here, is directed at questions concerning the representation and role of the overflow processes, with respect to the formation and transport of NADW and to the simulation of the NAC. In a subsequent study the model, with an optimized choice of inflow conditions and parameterizations, will be applied to study aspects of the seasonal cycle, subpolar mode water formation, and the effects of deep convection in the Labrador Sea.

Section 2 gives a description of the model configuration and an outline of the experiments. In section 3 we shall discuss the results of a series of test cases and sensitivity runs: a test of the southern boundary condition by comparison with a CME reference case (3.1), the effect of an open northern boundary with inflows and outflows compared to the buffer zone approach used in the CME (3.2), the effect of different inflow conditions in the Denmark Strait (3.3), the representation and role of the Faeroe Bank Channel overflow (3.4), and the combined effect of an open northern boundary and a modified channel topography on the circulation in the northeastern part of the basin (3.5). The results are summarized and discussed in section 4.

2. The Model

The numerical experiments are based on the primitive equation model developed at the NOAA Geophysical Fluid Dynamics Laboratory [*Bryan*, 1969], making use of the revised code (MOM-version 1.1) described by *Pacanowski et al.* [1993]. The model spans the Subpolar North Atlantic between 43° and 65°N, using the same grid configuration and, for the basic experiment, the same bottom topography as the model of the North Atlantic (from 15°S to 65°N) developed in the framework of the WOCE CME [*Bryan and Holland*, 1989]. The bottom topography of the CME was taken from a digital data set with 5' resolution. Except for removal of single grid point holes or spikes, no smoothing was applied.

2.1. General Description

A suite of experiments has been performed under the CME, aiming at the effects of horizontal resolution, friction coefficients, wind forcing and thermohaline boundary conditions. For a list of CME experiments and parameters, the reader is referred to *Bryan et al.* [1995] and *Böning et al.* [1996]. For the regional model experiments described here we have adopted a horizontal grid spacing of $1/3° \times 2/5°$ (meridionally × zonally). Previous studies had shown that this grid, because it resolves only the uppermost range of the the mesoscale eddy spectrum, significantly underestimates the eddy energy in the subpolar basin [*Böning and Budich*, 1992; *Beckmann et al.*, 1994b]. However, for many aspects of the mean circulation, it may be considered as a reasonable compromise: CME experiments with this grid spacing revealed major improvements compared to a non-eddy-resolving ($1° \times 1.2°$) version [*Böning et al.*, 1996] but only small differences compared to a very high resolution version with a $1/6° \times 1/5°$ grid [*Beckmann et al.*, 1994a]. Horizontal mixing is parameterized by biharmonic friction, and we use constant coefficients for both viscosity and diffusivity of 2.5×10^{19} cm^4/s.

In the vertical there are 30 discrete levels, with a spacing of 35 m at the surface and smoothly increasing to 250 m at 1000-m depth. Below 1000 m the vertical grid box thickness is a constant 250 m; the maximum depth is 5500 m. Constant Laplacian mixing is used with coefficients of 0.3 cm^2/s for diffusion and 10 cm^2/s for viscosity. If the stratification of a water column is unstable, the effect of free convective overturning is parameterized by increasing the vertical diffusion coefficient to 10^4 cm^2/s. Wind-forced deepening of the surface layer is included by a one-dimensional *Camp and Elsberry* [1978] type mixed layer model.

The thermohaline boundary conditions at the sea surface follow the CME formulation. The haline boundary condition is given by a linear damping of the surface salinity toward the seasonal climatology of *Levitus* [1982]. The thermal boundary condition is specified by a linear bulk formula [*Haney*, 1971] which calculates the air-sea heat flux from the difference between the model-predicted surface temperature and a prescribed, "effective" atmospheric temperature derived from various monthly mean climatological data sets following [*Han*, 1984]. This formulation differs from the one adopted in other model studies, e.g., *Sarmiento* [1986], *Semtner and Chervin* [1992] and *Roberts and Wood* [1997], which used a damping toward the monthly mean *Levitus* [1982] temperature. In order to examine the effect of this difference, our sequence of experiments (see below) includes a sensitivity run with a similar thermal boundary condition. As in the CME, the effect of sea ice on the thermohaline fluxes is accounted for by an additional damping of temperature (Θ) and salinity (S) along the Labrador shelf, north of Hamilton Bank, towards the monthly mean values of *Levitus* [1982]. For the dynamical boundary condition at the sea surface, all experiments use the monthly mean wind stress climatology of *Isemer and Hasse* [1987].

For the open southern boundary at 43°N a scheme allowing inflow and outflow has been devised that follows the approach developed by *Stevens* [1991] for the Fine-Resolution Antarctic Model (FRAM) of the Southern Ocean [*FRAM Group*, 1991]. An ideal open boundary condition is transparent for waves moving towards the

boundary, with no reflection of wave energy back into the model. For ocean models this problem is ill posed [*Bennet and Kloeden*, 1981]: it is not possible to define a set of equations that exactly match the characteristics of the solution from the interior at the boundary.

In the approach adopted here the open boundary problem, unless still ill posed, works sufficiently well as will be demonstrated in section 3.1. The vertically integrated volume transport is prescribed along the boundary, while the vertical shear is left free to adjust. The distribution of inflow and outflow points along the section is thus not given a priori but determined by the dynamics of the model. Since the barotropic circulation at 43°N is not known with sufficient accuracy from observations, the volume transport is taken from a CME reference case (experiment K13-2 [*Böning et al.* ,1996]). The same CME solution provides the temperature and salinity data needed at inflow points. More specifically, we use seasonal mean CME data, linearly interpolated to the actual time step of the model integration, and a damping of the inflow data toward these values with an inverse timescale of $1/25\ d^{-1}$. At outflow points the model is able to advect the tracers onto the boundary using a simplified advection-diffusion equation to approximate the unknown solution at the open boundary. No additional damping close to the open boundary was necessary to obtain stable solutions. A more detailed description of the open boundary conditions is deferred to the Appendix.

For the northern boundary at 65°N, two different techniques are used. In one set of experiments the same condition as in the CME is adopted; that is, the boundary is closed to normal flow, and tracer values are damped toward observed data within a narrow (four grid boxes width) "buffer" zone adjacent to the boundary. In the other set of experiments, the northern boundary between Greenland and Norway is open. The methodology is basically the same as for the open southern boundary, except that the volume transport and tracer values cannot be taken from a model solution. Due to the limited quantitative knowledge of the vertically-integrated transport, there is no dynamically consistent set of observational data available so that there is some ambiguity in the specification of the conditions here. Transport schemes advanced in the literature show total northward transports between Iceland and Norway of 4 to 6 Sv [*Schmitz and McCartney*, 1993; *Krauss*, 1986] For the present experiments, a zonal distribution of the streamfunction has been devised, with an inflow of 5.6 Sv between Greenland and Iceland and a corresponding outflow between Iceland and Norway (see Figure 6a, top).

Temperature and salinity at inflow points are taken from two different data sets. One is based on the *Levitus* [1982] climatology. The other is the same except for deep levels (below 1400 m) in the Denmark Strait, where the smooth climatology is replaced by actual section data that include the signature of Denmark Strait Overflow Water (DSOW). The data sets that are used in the present study for the restoring of the tracer values at inflow points are the same as those used for the northern buffer zone of the CME [*Döscher et al.*, 1994]; for details and plots of the section data the reader is referred to that paper.

The need to specify the tracer values at inflow points and the barotropic stream function implies that a regional model is not meaningful for long integration times. The CME experiments as well as a similar study by *Gerdes and Köberle* [1995] have demonstrated that the dynamical response to changes in the northern thermohaline boundary conditions involves an adjustment of the basin-wide overturning circulation on a time scale of about 10 to 15 years [*Döscher et al.*, 1994].

However, due to the Joint Effect of Baroclinicity and Relief (JEBAR) this will eventually affect the horizontal mass transport stream function [*Greatbatch*, 1991], a mechanism that at the southern boundary of the regional model is prevented by the form of the boundary condition. The problem may be somewhat alleviated by the choice of 43°N for the southern boundary since the CME analysis of *Döscher et al.* [1994] showed a comparatively weak response of the horizontal stream function in this intergyre regime. In general, however, a regional model (in fact, any model with less than global coverage) is not a perfect tool to study the long-term, equilibrium behavior of the circulation. Instead, the experiments presented here are primarily concerned with the deviations of the three-dimensional flow field in the northeastern basin from a CME solution in quasi-dynamic equilibrium, which are caused by perturbations in a number of model factors, in order to contribute to an understanding of their role in the thermohaline circulation.

2.2. Experimental Strategy

All experiments with the regional model are initialized with the mean state of CME case K13-2, i.e., the same model solution that provides the southern boundary data. More specifically, the regional model runs were started with a 5-year average of winter Θ and S and zero velocities. Table 1 gives an overview of the experiments. The results presented in this study are based on 1-year annual mean values.

In a first step, the effect of the open southern boundary at 43°N and the ability of the regional model to reproduce the solution of the CME for the subpolar area are tested. Experiment R1 uses the same northern boundary condition, i.e., a closed wall and restoring to the Levitus climatology, as the CME reference case.

In experiment R2 the bottom topography of the Iceland-Scotland Ridge is modified to examine the effect of an increased outflow of Norwegian Sea Water into the Iceland Basin. In the original CME model topography the Faeroe Bank Channel, which lies south of the northern buffer zone, was not wide enough (i.e., of only

Table 1. List of Experiments With the Regional Model

Experiment	Northern Boundary	Northern Restoring/ Inflow	Faeroe Bank Channel	Integration Period, years	Surface Forcing
R1	closed	Levitus	narrow	15	Haney
R2	closed	Levitus	wide	6	Haney
R3	open	Levitus	narrow	6	Haney
R4	open	Levitus	wide	6	Haney
$R4^{Lev}$	open	Levitus	wide	6	Levitus
R5	open	section	wide	6	Haney

one grid box width) to allow an advective flux of water on the model B grid. In order to enable an exchange of water down to a depth of about 900 m, the channel is widened artificially to two grid boxes (minimum).

The effect of an open northern boundary with inflow and outflow through the Greenland-Iceland and Iceland-Norway sections is examined in experiment R3 which is otherwise identical to R1 and thus the CME reference case. The combination of an open boundary with a widened Faeroe Bank Channel is examined in experiment R4. The effect of different inflow conditions for Θ and S is tested in experiment R5 in which the Levitus climatology for Denmark Strait inflow points is replaced by the modified climatology of *Döscher et al.* [1994] that incorporates the signature of the narrow core of cold (0° to 1°C) DSOW.

The sensitivity of the NAC against changes in thermohaline surface forcing is examined in experiment $R4^{Lev}$, motivated by a number of model studies that used a restoring to monthly mean sea surface temperatures [*Semtner and Chervin*, 1992] and showed a course of the NAC very different from the CME that used a Haney condition. In $R4^{Lev}$ we repeated experiment R4 with a modified heat flux formulation, i.e., restoring to Levitus SSTs on a timescale of 30 days.

Finally, experiments R1 to R2 were repeated (not shown in Table 1) by setting the stream function along the southern boundary to zero, in order to study the sensitivity of the regional model to the barotropic forcing at the open southern boundary.

3. Results

3.1. Test of the Southern Boundary Condition

Before using the regional model for an examination of the role of different model factors in simulations of the subpolar circulation system, we want to assess its ability to mimick the regional behavior of the basin-wide CME model. Experiment R1 was integrated with the same surface and northern boundary conditions as the CME reference case. In the following, the flow structure averaged over the last (fifteenth) year of integration is compared to the mean flow structure of the reference case.

We begin with a look at integrated quantities. As shown by the zonally integrated stream function displayed in Figure 2 the models differ very little in the net meridional overturning. In particular, there is hardly any indication, in an integral sense, of an energy reflection at the southern boundary of the regional model.

For an intercomparison of the horizontal flow pattern we will focus on an upper level (175 m) representative for the structure of the NAC. A robust feature in all CME models is a NAC whose main branch turns northward west of the MAR and flows toward the Denmark Strait (Figure 3a). Part of the flow is deflected westward in the Irminger Sea to feed the East Greenland Current, and part is sinking and returning at depth. The circulation in the Labrador Sea includes a cyclonic gyre whose main current core roughly follows the 2500-m isobath and a shallow current on the Labrador shelf. The basic flow structure is well reproduced in the regional model (Figure 3b). There is not only a close correspondance in the major aspects of the subpolar gyre, e.g., the course of the NAC or the presence of a shallow and a deep branch of the Labrador Current, but also in the weaker flow patterns in the eastern basin, close to the open southern boundary, e.g., in the Bay of Biscay. Differences in flow details near the southern boundary can be attributed to the absence of eddy propagation into the model domain due to the use of time mean and hence smooth values for the stream function and tracer values for inflow points.

The deep flow structure in the two models is compared in Figures 3c and 3d for a level (1800 m) representative of the circulation of NADW. The most pronounced difference occurs along the southern boundary in the eastern North Atlantic. The eddy signal visible in the regional model (Figure 3d) can probably be attributed to a partial reflexion of energy at the boundary.

Apart from that, both models show a similar structure of the Deep Western Boundary Current (DWBC). In these cases the model NADW characteristics are mainly set by the damping to prescribed climatological values in the buffer zone between Greenland and Iceland. The bulk of the sinking of upper layer, NAC water occurs in the Denmark Strait buffer zone and near the Reykjanes Ridge south of Iceland [*Böning et al.*,

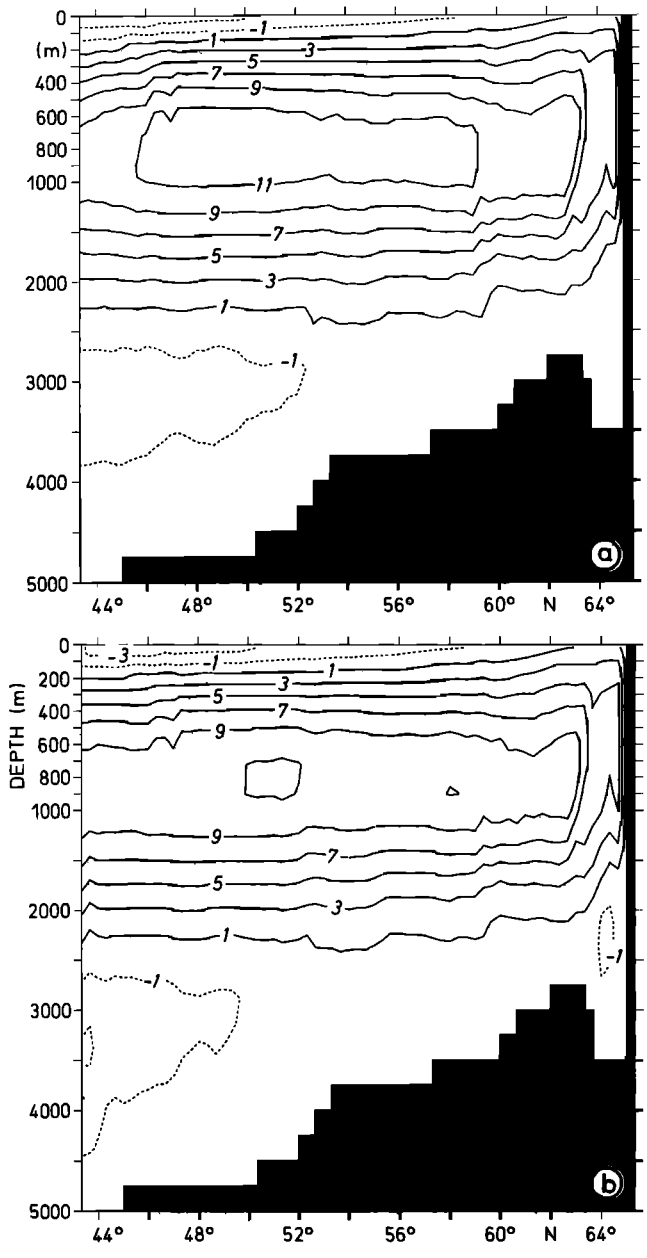

Figure 2. Annual mean of the zonally integrated meridional stream function in sverdrups for experiments (a) K13-4 and (b) R1; the contour interval is 2 Sv.

1996; *Ernst*, 1995]. Both models show a similar structure of the DWBC. around the Irminger and Labrador Basin. This includes the unrealistic separation from the Labrador continental slope and eastward deflection at about 52°N, just north of the overlying subarctic front. In both cases, there is an anticyclonic circulation of deep water in the Newfoundland Basin, with the main southward flow along the MAR, not along the Grand Banks. The flow re-attaches to the western boundary south of Flemish Cap, just north of the southern boundary of the regional model. The cause of this eastward deflection of the DWBC, for example, whether it is related to the unrealistic northward flow of the NAC through Flemish Pass pointed out by *Böning et al.* [1996], is the scope of ongoing research using higher-resolution models, with a different realization of the local topography.

A more quantitative look at the volume transports is provided with Figure 4, showing the zonal flow through a section along 44°W, between Cape Farewell and Flemish Cap. The density and velocity distribution illustrates a weakly depth-dependent boundary current; its transport between Cape Farewell and roughly 56°N is 20.1 Sv for the CME reference case K13-4 (Figure 4a) and 18.8 Sv for the regional model (Figure 4b). The agreement is remarkably close given the strong sensitivity of this measure of the strength of the subpolar gyre to various model factors as noted by *Böning et al.* [1996].

The structure of the meridional flow along 43°N is shown in Figure 5. The gross distribution of areas with northward and southward flow is similar in both cases. However, there are differences in some details of the flow. An example is the more noisy pattern east of 40°W in the regional model (Figure 5b), possibly indicating some reflection of energy at the artificial boundary but without affecting the basin-wide thermohaline circulation.

The prescription of the stream function at the southern boundary of the regional model seems to be of little consequence to the intensity of the thermohaline circulation in the subpolar basin: setting the stream function to zero along 43° only resulted in a decrease of the meridional overturning by about 1 Sv. This behavior indicates once more the weak influence of barotropic forcing on the thermohaline circulation (a result that has been noted earlier in CME experiments using different wind stress climatologies).

In summary, the results of the test case R1 demonstrate a general ability of the regional model to reproduce the main flow patterns obtained with the full North Atlantic model. In the response experiments described below, the model is used to elucidate the role of individual model factors in simulations of the subpolar circulation.

3.2. Effect of Open Northern Boundaries

A potential problem of the closed boundary and buffer zone approach concerns the horizontal structure of the subpolar gyre, in particular, the tendency of the NAC to flow north in the Irminger Basin, west of the MAR. This may be attributed to two aspects of the buffer zone configuration adopted in the CME and our test case R1: first, the meridional exchange of water between the Norwegian and Iceland Basins is small due to the blocking effect of the Iceland-Scotland Ridge, which, in the original implementation, lacks a deep passage for advective flux; second, the presence of Iceland prevents a zonal redistribution of water within the buffer zone. The effect of these factors on the subpolar circulation will be examined in two steps. One is the introduction of open

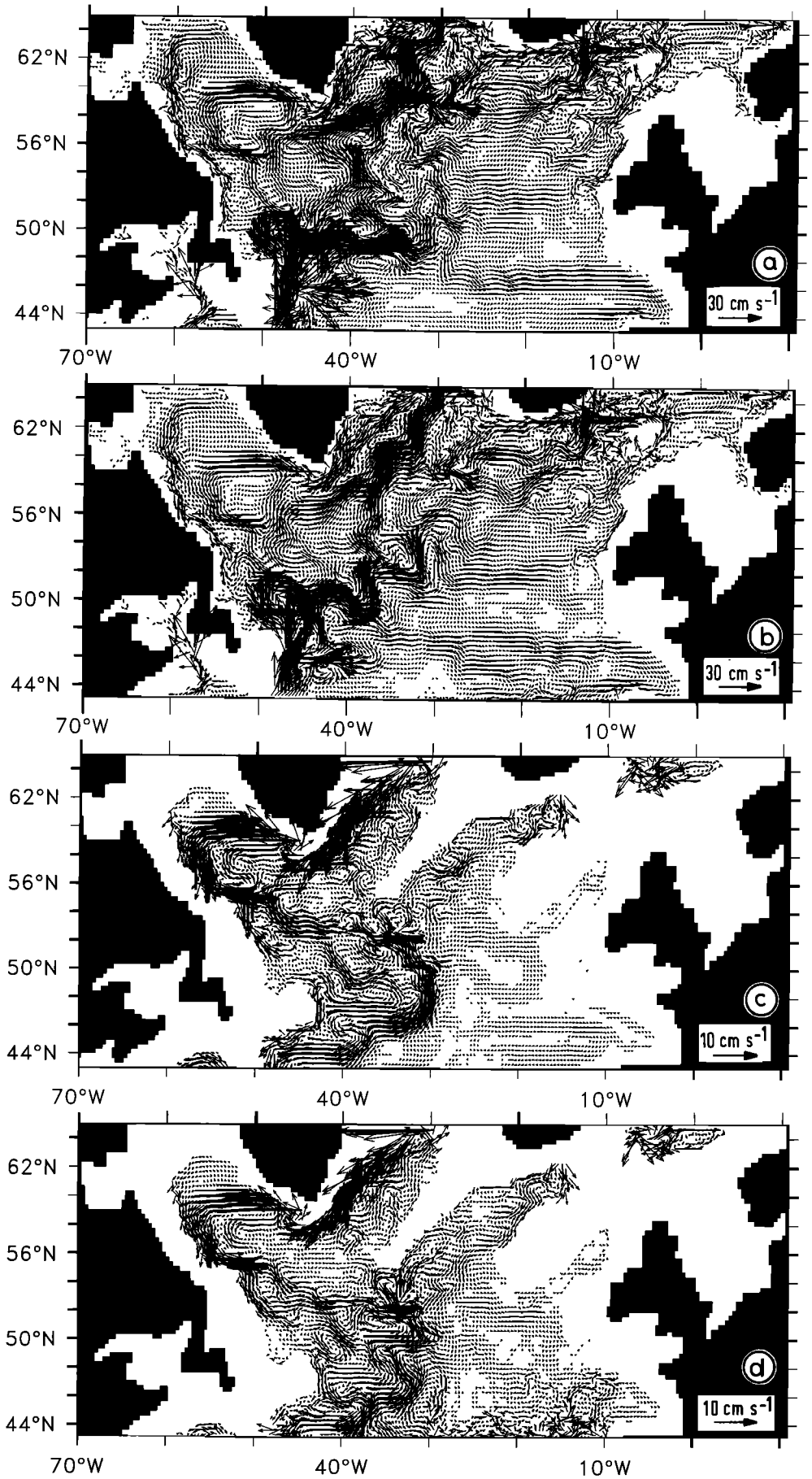

Figure 3. Annual mean horizontal velocity in centimeters per second at level 5 (175 m) for (a) CME experiment K13-4 and (b) R1, and at level 16 (1800 m) for (c) K13-4 and (d) R1.

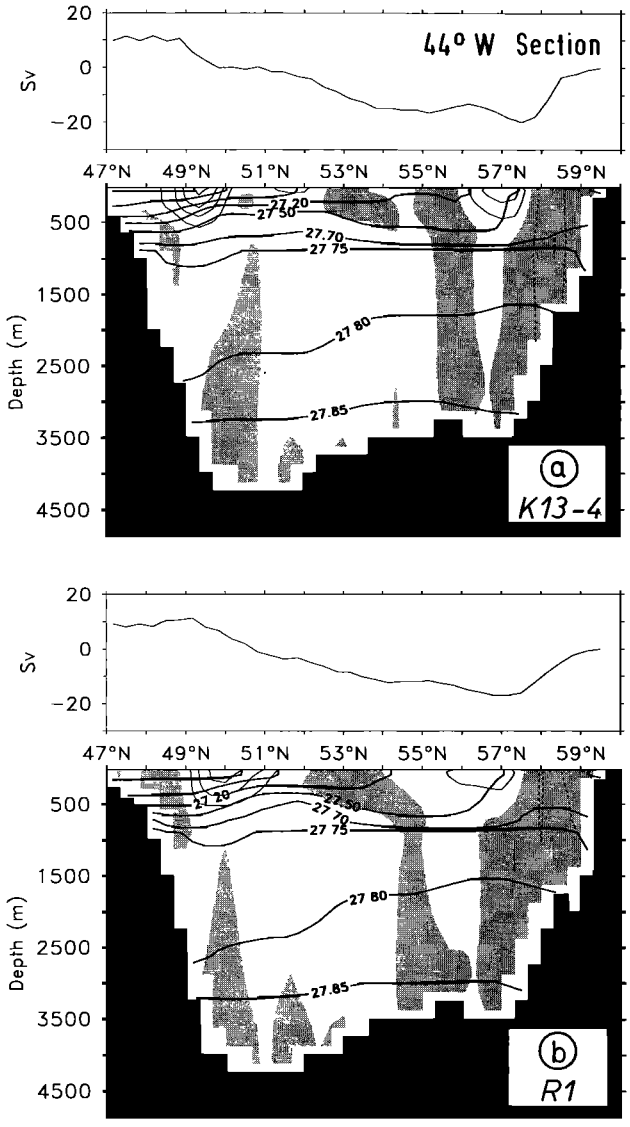

Figure 4. Meridional section along 44°W from Flemish Cap to Cape Farewell of annual mean values of σ_Θ overlayed on zonal velocity, with the vertically integrated transport shown at the top for (a) K13-4 and (b) R1. The contour interval is 0.3 σ units for $26.0 \leq \sigma_\Theta \leq 27.5$ and 0.05 σ units for $\sigma_\Theta \geq 27.7$; the contour interval for velocity is 5 cm/s. Areas with westward velocities (negative values) are shaded.

northern boundary conditions, with a net outflow between Iceland and Norway, compensated by an inflow between Greenland and Iceland. A version with Θ and S inflow conditions taken from the Levitus climatology is described in this section, a version with inflow data for the Denmark Straits based on an actual section is described in section 3.3. The other is a widening of the Faeroe Bank Channel to allow a throughflow down to depths of 900 m, described in sections 3.4 and 3.5.

The stream function of the vertically integrated flow prescribed at the northern boundary is shown in Figure 6a (top, thick line) for R3. There is a total outflow of 5.6 Sv east of Iceland and a total inflow of 5.6 Sv through Denmark Strait, between 28° and 40°W. The dynamical adjustment of the baroclinic flow through the open boundary mainly takes place during the first 4 years of the integration, after which changes in the flow structure are small. The zonal cross section of Figure 6a (bottom) gives the mean values of potential density (σ_Θ) and meridional velocity for the final (sixth) year of the response experiment. Despite the smooth, monotonous structure of the stream function, both segments of the section contain inflow as well as outflow points. Over the Denmark Strait, outflow is confined to a narrow strip near 32°W, with surface velocities reaching 4 cm/s. The rest of the section is dominated by inflow with typical velocities of 1 to 2 cm/s. Maximum southward velocities, up to 16 cm/s, occur over the shelf west of 33°W, representing the model equivalent of the East Greenland Current. In the eastern

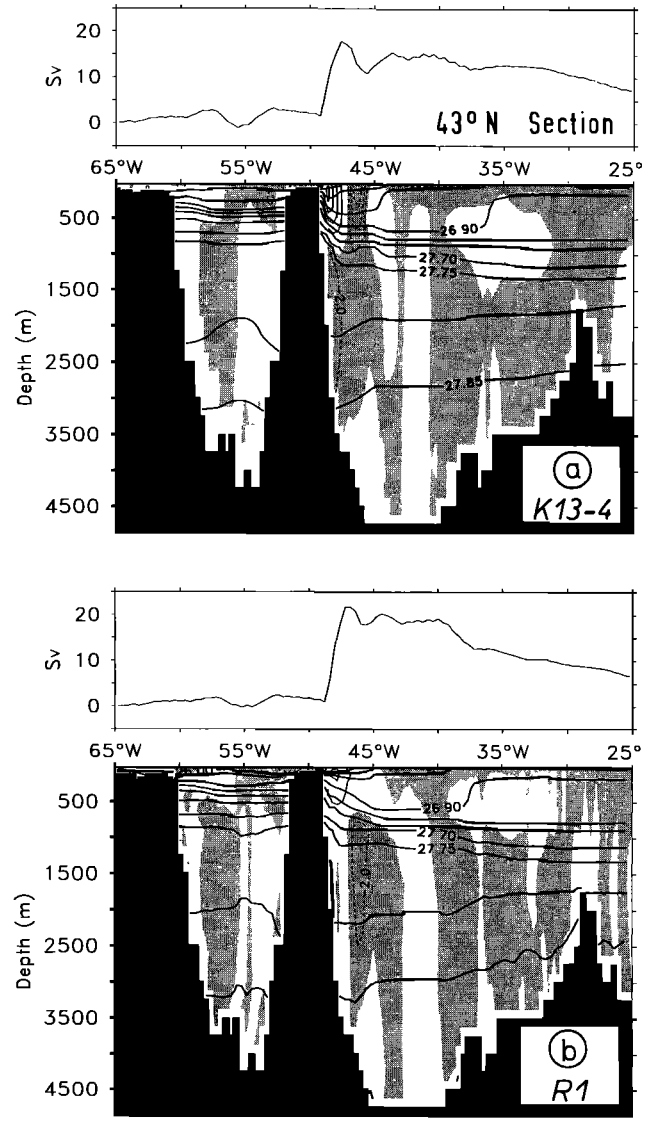

Figure 5. Like Figure 4, but along 43°N from Newfoundland to the Mid-Atlantic Ridge. The contour interval for northward velocity (solid lines, positive) is 10 cm/s; for southward velocity (dashed lines, shaded areas) it is 2 cm/s.

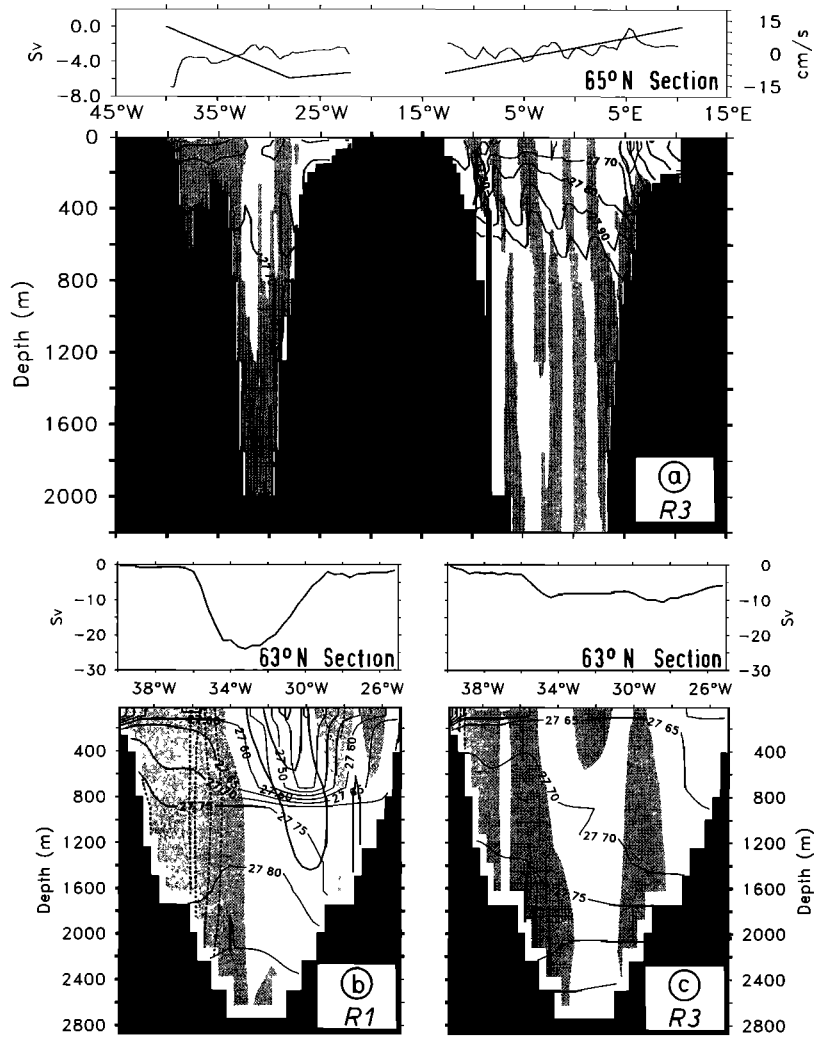

Figure 6. (a) Section plot along 65°N of annual mean values of σ_Θ and meridional velocity along the open boundary for experiment R3 between Greenland and Norway, vertically integrated transports (thick line), and meridional velocity at 50 m (thin line) on top. The contour interval for velocity is 5 cm/s. Shaded areas indicate southward velocities. Here σ_Θ is contoured with an interval of 0.20 σ units between σ_Θ =26.0 and σ_Θ =27.6 and 0.10 σ units between σ_Θ =27.6 and σ_Θ =28.0. Section plots along 63°N in the Denmark Strait for (b) R1 and (c) R3; contour spacing is 0.05 units for σ_Θ and 5 cm/s for velocity. Areas with southward velocities are shaded.

segment, the outflow is concentrated at 5°E, but there are also wide areas with an inflow of water mainly at depths below 1000 m.

Figures 6b and 6c give a comparison of model cases R1 and R3 across the Denmark Strait at 63°N. There is a strong difference in the meridional velocity structure. In the closed boundary case R1, there is an intense (nearly 25 Sv) barotropic recirculation in the northern Irminger Basin, with northward, surface-intensified flow along the MAR and southward, weakly depth-dependent flow along the Greenland continental slope. The northward current represents the extension of the NAC being drawn into the buffer zone; it is associated with the advection of warm water from the south and the establishment of a strong pycnocline at about 800 m. This spurious current signal vanishes in the open boundary case R3. In that case we find a net southward transport of 10 Sv over the section, the bulk of it concentrated near 35°W where it is associated with the bottom-intensified flow of dense water from the northern boundary. It is interesting to note that the smooth, artificial stream function profile prescribed at 65°N develops into a more structured, apparently more realistic pattern only three grid boxes farther south. The increase of southward transport is made of water flowing northward along the Reykjanes Ridge but more to the east compared to R1.

Despite these differences near the northern boundary, inspection of a horizontal map of the velocity field in R3 analogous to Figure 3b reveals little differences in the overall course of the NAC (not shown therefore): in particular, there is still a tendency for the bulk of the surface current to extend northward toward Denmark Strait, instead of a northeastward continuation. Hence,

regarding the simulation of the subarctic front and the corresponding NAC pattern in the northeastern basin, the conclusion at this point is that the opening of the northern boundary alone is not sufficient to obtain a more realistic simulation of the upper layer circulation.

A most critical issue in modeling the North Atlantic thermohaline circulation is the density of the deep water invading the basin from the north. In the real ocean, DSOW represents the densest source component of NADW, with potential densities of $\sigma_\Theta = 27.95$ to $\sigma_\Theta = 28.0$ [*Strass et al.*, 1993] within the Denmark Strait. The core of the outflow descends along the Greenland continental slope from 600 m at 67°N to 3000 m at 60°N [*Swift*, 1984]. The CME sensitivity studies have demonstrated the decisive influence of the model representation of the deep water characteristics near the northern boundary, on the strength of the meridional overturning cell as well as on the vertical distribution of the southward flowing, deep branch [*Döscher et al.* 1994; *Holland and Bryan*, 1994; *Böning et al.*, 1996] For both cases considered here, the water mass characteristics supplied by the northern boundary conditions deviate from the observed DSOW characteristics due to the use of the smoothed, climatological data. The effect of actual section data as inflow condition at the open boundary will be examined in the following subsection. Apart from this general deficiency, there is an important difference between the deep density and current patterns of the 63°N sections displayed in Figure 6b. In the open boundary case R3 the abyssal density has decreased by about 0.05 σ units, the 27.75 σ surface being approximately 400 m deeper than in R1. A similar difference holds for the density advected southward by the deep boundary current. Along with that we notice a shoaling of its core, from about 2200 m in R1 to 1800 m in R3. Consistent with the strong sensitivity of the subpolar basin circulation found in the CME (compare Tables 2 and 3 of *Böning et al.* [1996]), the net deep water formation in the subpolar basin, measured by the zonally integrated outflow across 43°N, decreases from 11 Sv (R1) to 7.5 Sv (R3), while the current observational picture, as summarized by *Schmitz and McCartney* [1993], gives values of about 13 Sv. Corresponding to the decrease in deep water formation, the horizontal gyre transport weakens as revealed, for example, by the westward transport of the boundary current off Cape Farewell (Table 2). The difference in the outflow properties between the open and closed boundary cases has mainly to be attributed to the spurious, diapycnic mixing affecting the dense outflow near the northern boundary, which will be examined further in subsection 3.3.

3.3. Sensitivity to Denmark Strait Inflow Conditions

Experiments R4 and R5 use the same open boundary conditions at 65°N except for the Θ and S data adopted at inflow points. Both cases use the modified Faeroe Bank Channel topography whose effect will be discussed in section 3.4.

Figure 7 shows the mean flow structure across 65°N, between Greenland and Iceland. The velocity patterns obtained in the two cases are similar over the shelf areas on both sides of the channel for these two experiments; for example, the southward transport of the East Greenland Current, west of 35°W, is 2.5 Sv in both model versions. A strong difference, however, occurs over the central, deep portion of the section. The core of the deep southward current is much narrower in R5 (Figure 7a), and is pressed against the continental slope on the western side. Maximum velocities at the bottom are 34 cm/s in this case, compared to 8 cm/s in R4 (Figure 7b). The transport of the deep inflow, below 1000 m depth, increases from 2.1 Sv in R4 to 9.0 Sv in R5. A quantitative validation of this transport against observational numbers is not straightforward: the 65°N section is already south of the Denmark Strait sill for which *Dickson and Brown* [1994] cite a value of 2.9 Sv for the overflow, and it seems plausible that the bulk of the increase to the 10.7 Sv as observed near 63°N should

Table 2. Transport of the Boundary Current off Cape Farewell, Across 44°W, and Transport Through a Section Along 7°W, From 58° to 62°N, West of the Faeroe Bank Channel Sill

	Cape Farewell		Faeroe Bank	
	Upper Layer	Lower Layer	Upper Layer	Lower Layer
	Observations			
Clarke [1984]*	-14.0	-19.5		
Saunders [1990]†				-1.9
	CME			
K13-4	-9.5	-10.6	2.5	-0.1
K13-6	-23.3	-16.3	2.5	-0.1
	Regional Model			
R1	-8.7	-10.1	2.5	-0.3
R2	-7.6	-10.4	5.1	-4.4
R3	-6.1	-6.1	3.0	-0.2
R4	-7.7	-7.1	4.9	-2.5
R5	-12.0	-17.0	5.2	-2.6

Transport values are given in sverdrups. For an example of the current structure and section geometry see Figure 4. (Negative values indicate westward transports.) The upper layer is defined as 0 - 600 m; the lower layer is defined as 600 m to bottom for experiments with the wide channel and 0 - 400 m and 400 m to bottom for cases with the narrow channel.

* Upper layer components are the East Greenland Water and Irminger Water; the lower layer components are composed of North Atlantic Deep and Bottom Water of *Clarke* [1984].

† Transport of water colder than 3 °C.

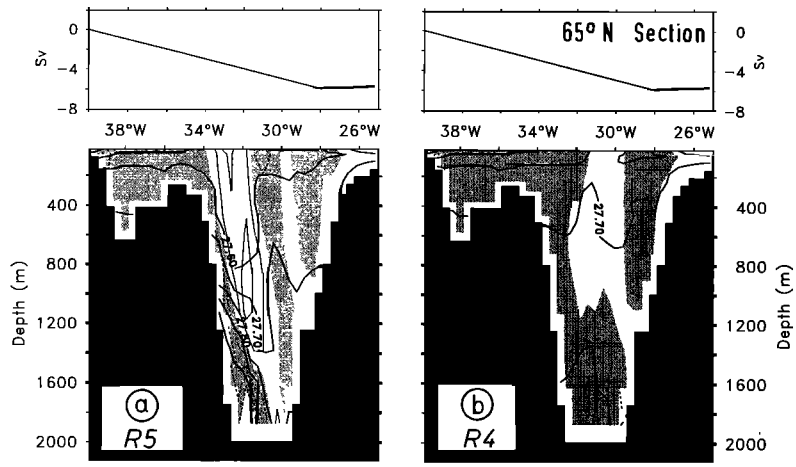

Figure 7. Section plot along 65°N in the Denmark Strait for (a) R5 and (b) R4; contouring is as in Figure 6a. Areas with southward velocities are shaded.

occur just south of the sill. Hence one may argue that a boundary condition at 65°N should not reproduce the conditions at the sill, but rather account for the effect of the entrainment processes to the south of the sill, north of the model domain. Because of the fixed stream function at the northern boundary, the stronger deep flow in R5 is associated with a simultaneous increase in the upper layer, northward flow over the southern Denmark Strait. While the particular structure of the model Irminger Current is obviously strongly affected by the artificial choice of the stream function, the underlying reason for its existence, that is, the feeding of the increase in the deep transport south of the ridge, may not be unrealistic.

Another, but probably less important artifact of the open boundary condition is that the modeled inflow of dense water is subject to a pronounced annual cycle with an amplitude of more than 1 Sv, a signal not seen in the observations reported by *Dickson and Brown* [1994]. Its origin may probably also be traced to the lack of a consistent barotropic and baroclinic flow data set for the northern boundary. Since the stream function is held constant during the integration, any annual signal in the outflow produced by the seasonal forcing over the model domain must be compensated by a corresponding annual signal in the inflow at depth.

The difference in the annual mean inflow signal between R4 and R5 has strong consequences for the strength of the basin-scale circulation. The net deep water production in the subpolar basin, i.e., the deep outflow across 43°N, is 14 Sv in R5, up from 11 Sv in R4. The enhanced overturning is, again, associated with a stronger transport of the subpolar gyre, i.e., a boundary current of 29 Sv off Cape Farewell against 15 Sv in the case with climatological inflow data (Table 2). The horizontal gyre transport is weaker though (by nearly 25%) than in the CME experiment K13-6 [*Böning et al.*, 1996] forced with the same section data in its northern buffer zone. Two additional factors apparently play a role here: the different implementation of the Faeroe Bank topography (to be discussed in the following section) and the different implicit mixing along the northern ridge topography taking place in model versions with a closed and open boundary.

The effect of the implicit, diapycnic mixing on the properties of the deep overflow water and the quantitative difference of this spurious model process between a model with a closed boundary and buffer zone (CME case K13-6) and a model with an open boundary using the same restoring data for inflow points (R5) are illustrated in Figure 8, showing a succession of cross sections south of the boundary. In both model versions, the extremum in the core properties of the overflow water is rapidly eroded on its way south. The effect is strongest in R5, over the first few grid boxes adjacent to the boundary: its minimum temperature at depths of 1800 m at the East Greenland rise of 0°C at 64°N (Figure 8b) is raised to 2.5°C at 63°N (Figure 8d), that is, over only three grid boxes. Farther downstream, changes become much smaller, with an increase to 2.7°C at 62°N (Figure 8f). The reason for this change in the DSOW core characteristics is a strong, vertical mixing induced by the standard convective adjustment scheme used in the model. The principle problems of such a scheme, in combination with a step-wise discretization of bottom topography, when dealing with a downslope flow of dense water, have been pointed out in previous studies [*Gerdes*, 1993a; *Roberts and Wood*, 1997]. A possible solution to this problem in Bryan-Cox type circulation models is proposed by *Beckmann and Döscher* [1997], using a σ coordinate boundary layer approach for the bottom level to parameterize downslope currents.

At this point it is important to note that the effect is quantitatively very different in the model version with the closed boundary, because in the buffer zone approach the damping is distributed over a number of grid rows (in this case 4) adjacent to the boundary. Though by this method the core properties achieved

at the boundary itself are less extreme, hence less realistic (1.9°C in Figure 8a), a strong change as in the open boundary version is avoided because the restoring zone encompasses the critical region of the strong topographic gradient south of the sill and extends to a greater depth. This method apparently better maintains the core properties of the overflow water, yielding 1.0°C at 64°N (Figure 8b) and 1.6°C at 62°N (Figure 8e). Associated with that, it gives a greater depth for the DWBC forming at the western slope of the Irminger Basin. The difference in the DSOW properties is reflected in the net overturning strength, being 14 Sv in R5 and 16 Sv in the CME case.

3.4. Role of Faeroe Bank Channel Overflow

Observations suggest a transport for the outflow of cold (-1° to 0°C) water from the Norwegian Sea across the Iceland-Scotland Ridge of the same order as for the outflow of Arctic Intermediate Water through Denmark Strait. The transport scheme advanced by *Dickson and Brown* [1994] has a transport of 1.7 Sv through the deepest passage, the Faeroe Bank Channel (sill depth about 850 m), and an additional overflow of about 1 Sv through several notches in the Iceland-Faeroe Rise (mean sill depth 500 m). The outflows, modified by entrainment of North Atlantic water [*Price and Baringer*, 1994], are believed to be collected by a deep boundary current along the Reykjanes Ridge and should enter the Irminger Basin mainly through the Gibbs Fracture Zone; however, transport numbers are still under debate [*Saunders*, 1994].

Concerning the problem of the numerical representation of this important source water mass for NADW in large-scale circulation models, one may distinguish two main aspects. The principle problem of simulating the overflow of a ridge in models that are not resolving the local Rossby radii has been discussed extensively by *Gerdes [1993a; 1993b]*. These models cannot generate shear vorticity to balance the local Coriolis forcing, and friction and diffusion become important for the flow across topographic barriers.

The other aspect, particularly relevant to (marginally) eddy-resolving models, has received comparatively little attention: the difficulty of representing the main conduit for the dense water from the Norwegian Sea, that is, the narrow and winding Faeroe Bank Channel. The effects of different realizations of the channel throughflow, obtained by modifications in the discretized bathymetry, are examined in the following.

Figure 9a shows the channel bathymetry as given by the ETOPO5 data set [*National Geophysical Data Center*, 1988], with 5'-resolution. In a straightforward discretization, as in the case of the original CME adaptation that was used also in the regional model versions R1 and R3, the deep portion of the narrow passage is not resolved on the grid on which the horizontal velocities are carried in the numerical model. With its mesh

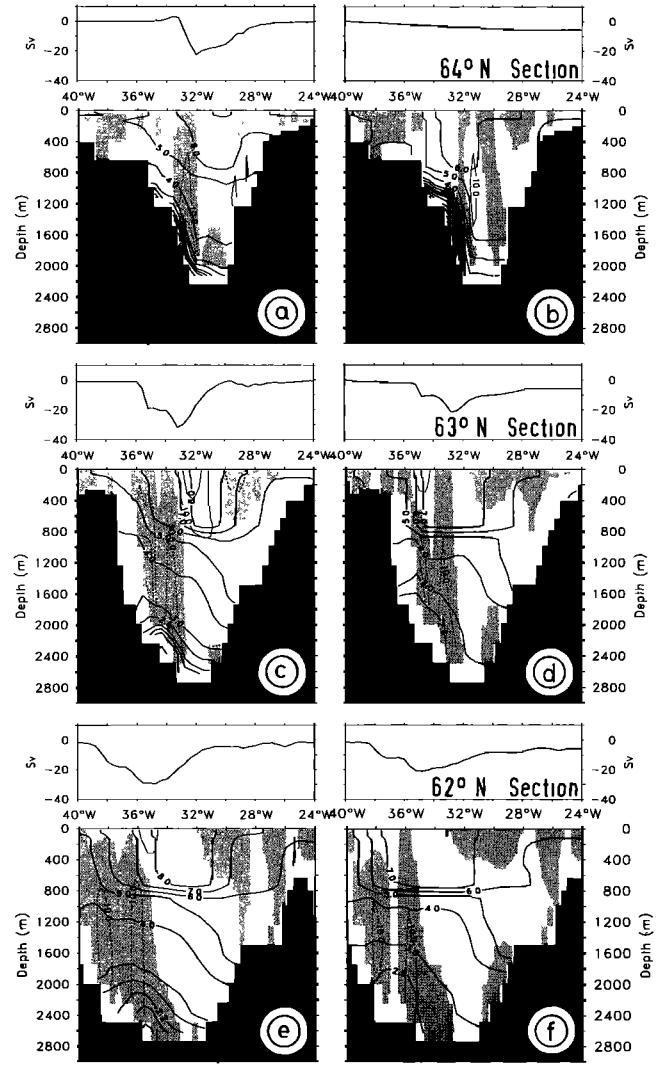

Figure 8. Annual mean values of potential temperature and meridional velocity, with the vertically integrated transport indicated at the top for experiment K13-6 at (a) 64°N, (c) 63°N and (e) 62°N and experiment R5 at (b) 64°N, (d) 63°N, and (f) 62°N. The contour interval is 1°C for temperature above 3°C and 0.4°C for temperatures below 3°C; contour interval for velocity is 4 cm/s.

size of 18 × 37 km at this latitude, the model B grid just resolves the channel at tracer (T-) points down to a realistic depth of 900 m, but a nonzero velocity at u points is only possible in the upper 400 m. Because of the model's no-slip condition at side walls, a cross section has to be represented by at least three u points (two T grid boxes), in order to permit an advective flux of water.

Figures 9b and 9c illustrate two different discretizations of the channel bathymetry, each having its deepest tracer grid cell at 900 m, by showing the surface which separates velocity grid cells with nonzero velocities in the center from grid cells with zero velocities in the center. The original CME discretization (Figure 9b) (in the following referred to as "narrow channel") is character-

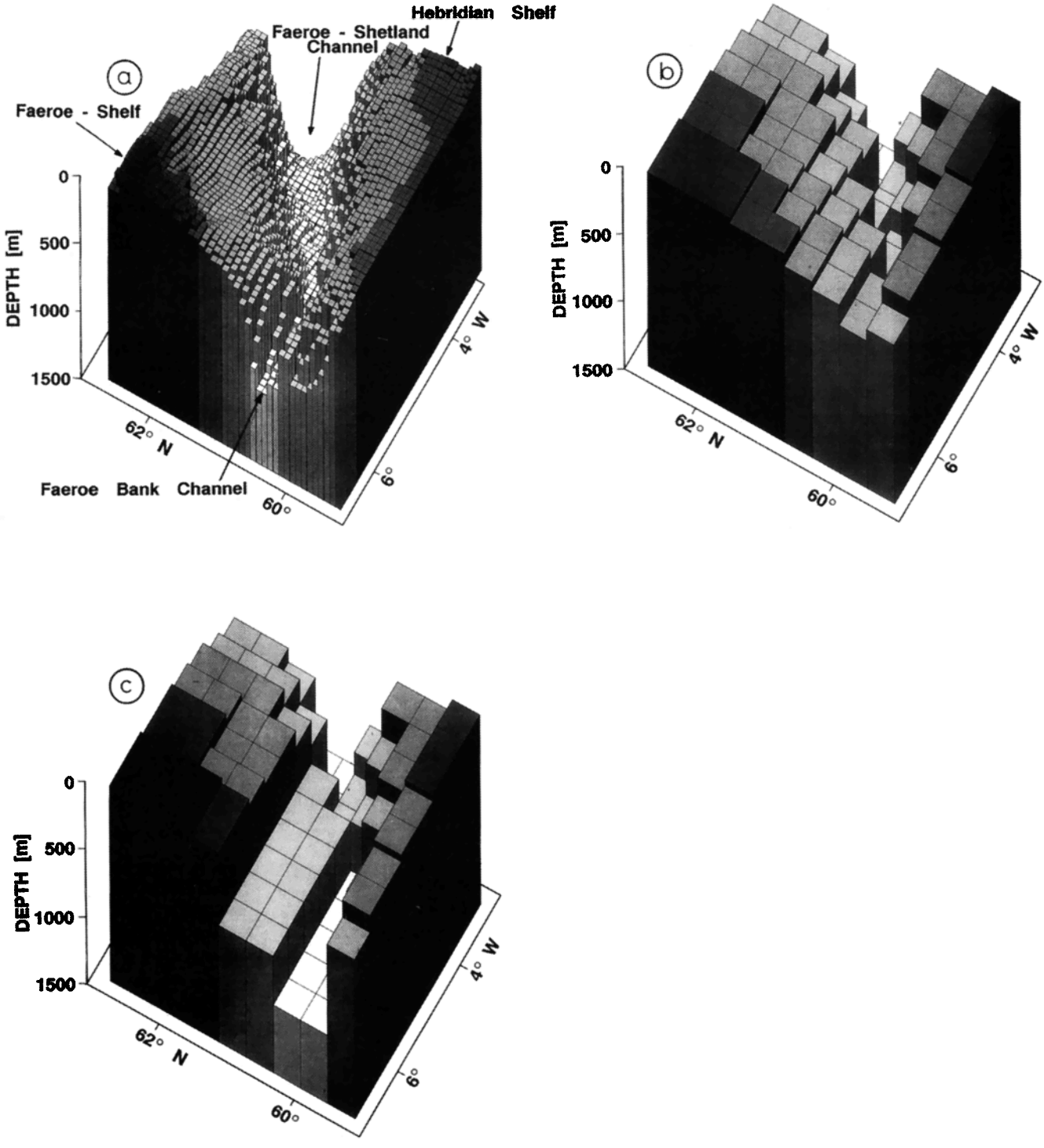

Figure 9. Topography in the region of the Faeroe Bank Channel (a) extracted from the ETOPO5 data set, (b) for velocity points in the CME model, and (c) for the experiments with a widened channel topography.

ized by zero velocities confined to depths below 400 m, since the deeper parts of the channel are resolved by only one tracer grid cell. Figure 9c shows the modified topography ("wide channel") used in R2, R4, $R4^{Lev}$, and R5, where the width of the channel has been artificially enlarged to a minimum of three tracer grid cells (corresponding to two nonzero velocity points), in order to allow an advective exchange of water down to the maximum depth of 900 m.

The effect of the widened passage is first assessed by comparing the closed northern boundary cases R1 (narrow) and R2 (wide) (Plate 1). The damping of temperature and salinity toward the Levitus climatology adjacent to the northern boundary produces a cold (less

than 0°C), homogeneous water mass north of the ridge fairly representative of the observed Norwegian Sea water characteristics. As shown by the 720-m pattern of horizontal velocity, an outflow of this water is effectively blocked in the narrow channel case R1 (Plate 1a). The mass transport through the deeper portion (below 400 m) of the Faeroe Bank Channel is negligible in all cases using the narrow channel geometry (Table 2). Accordingly, the middepth water mass characteristics south of the ridge are governed by the advection of temperate water from the south and the convective mixing (reaching to about 1000 m near the ridge) of the wintertime surface conditions over the Iceland Basin. Since the minimum surface temperatures south of the ridge, i.e., south of the arctic front, are not below 5° - 6°C, the blockage of an advective exchange of water results in a large temperature contrast across the ridge. The hydrography of the area becomes very different in R2 where the widened channel permits a significant outflow of Norwegian Sea water into the northeastern Iceland Basin (Plate 1b). The mass transport through the channel (near its western end, 7°W), for the depth range 600 m–bottom, exceeds 4 Sv in this case (Table 2).

A more detailed view of the current and temperature conditions along the channel is provided by a set of meridional cross sections shown in Figure 10. The first pair of sections (Figures 10a and 10b) shows the difference between R1 and R2 near the narrowest portion of the channel; the longitude (6°W) roughly corresponds to the western face of the channel block diagrams depicted in Figure 9. It should be noted that the topographic surfaces drawn in Figures 9 and 10 are defined in a different way. The cross sections show the bathymetry as defined in the usual way, by the side walls of the last "wet" tracer grid cells, i.e., the surface of zero velocity at the no-slip boundary, while Figures 9b and 9c focus on the topography of the nonzero velocity boxes. The distinction becomes clear especially by comparing Figure 9b with the cross-section of Figure 10a which shows the channel below 400 m to be resolved by just one tracer grid box in meridional direction. Because of the vanishing velocity at the side walls, there is no advective throughflow below 400 m, hence only an inefficient, diffusive spreading of cold water from the Norwegian Sea along the bottom of the channel. Comparison with the cross section of R2 (Fig-

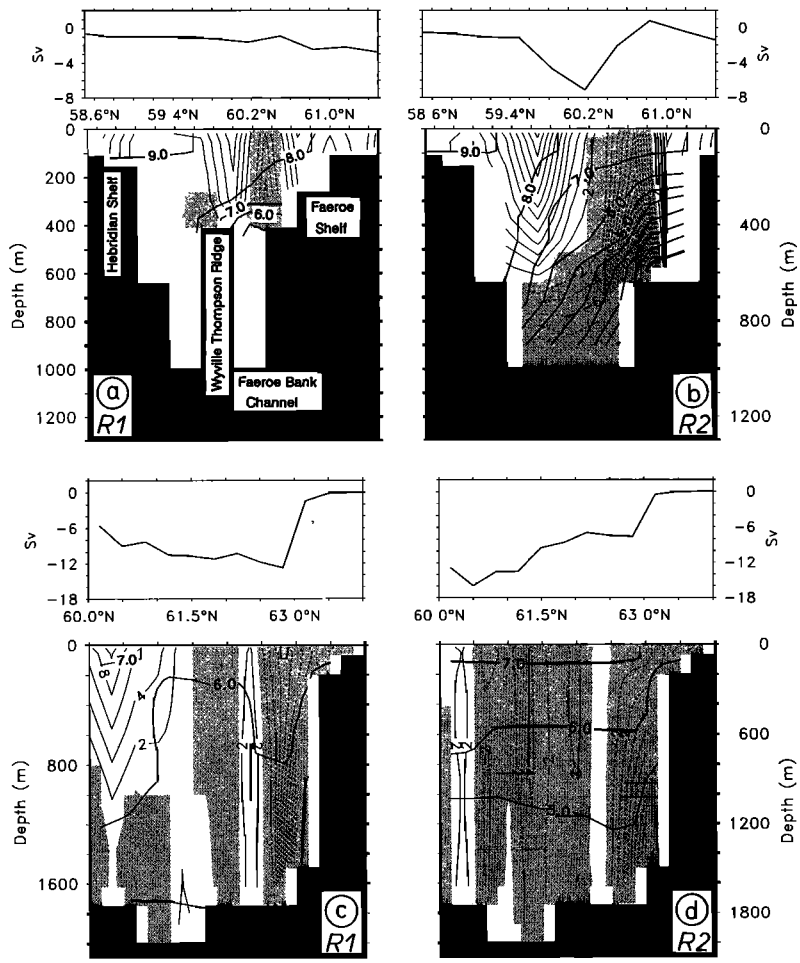

Figure 10. Annual mean potential temperature and zonal velocity at sections (a-b) along 6°W over the Faeroe Bank Channel and (c-d) along 14°W south of Iceland with stream function on top. Contouring for velocities is 2 cm/s; temperatures are contoured in 1°C intervals.

ure 10b) shows that the artificial widening of the channel at this site was mainly facilitated by a removal of the narrow Wyville-Thomson Ridge limiting the channel to the south. The widening results in a bottom intensified outflow pressed against the northern slope, with a maximum speed of about 30 cm/s.

Upon exiting the channel area, the tracer signature of the overflow water is gradually diminished in a similar way as in the case of the DSOW signal, that is, by the spurious diapycnic mixing accompanying a flow of dense water in a downslope direction. Figure 10d shows that the temperature of the water carried by the deep boundary current along the continental slope south of Iceland is 4° – 5°C. The decrease by about 1°C in the deep Iceland Basin compared to R1 (Figure 10c) should probably not be interpreted as a direct effect of the channel outflow but as an effect of the changed three-dimensional circulation in the Iceland Basin that is caused by the opening of the passage. In the CME cases with a blocked exchange over the ridge, the continental slope south of Iceland was characterized by a strong, localized sinking of upper layer water, feeding the deep, southwestward boundary current along the Reykjanes Ridge [*Böning et al.*, 1996; *Ernst*, 1995]. While a similar behavior is realized in the regional model cases with the narrow channel, the downwelling of warm NAC water masses south of Iceland ceases in the cases with the widened channel in which the deep boundary current is fed by the outflow from the Norwegian Sea. By eliminating the spurious sinking pattern in the northern Iceland Basin, the outflow in R2 has an indirect effect on the deep hydrographic structure, causing a cooling compared to R1 by 1° – 1.5°C along the Reykjanes Ridge. In the following we focus on the effects on the large-scale circulation, e.g., the transport of the DWBC and the path of the NAC.

A schematic picture showing the volume transport of the deep currents is given in Figure 11 for selected

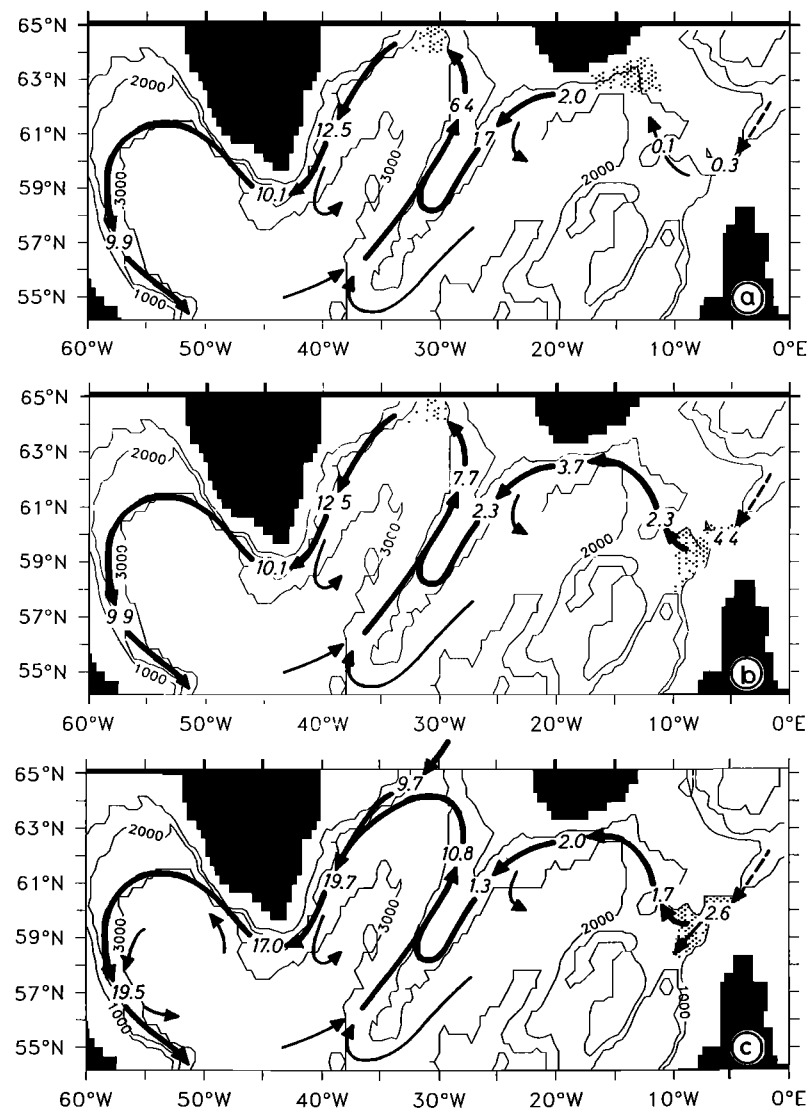

Figure 11. Schematic picture of the northern boundary current for experiments (a) R1, (b) R2 and (c) R5. Numbers indicate transports in sverdrups between 1000 m and the bottom.

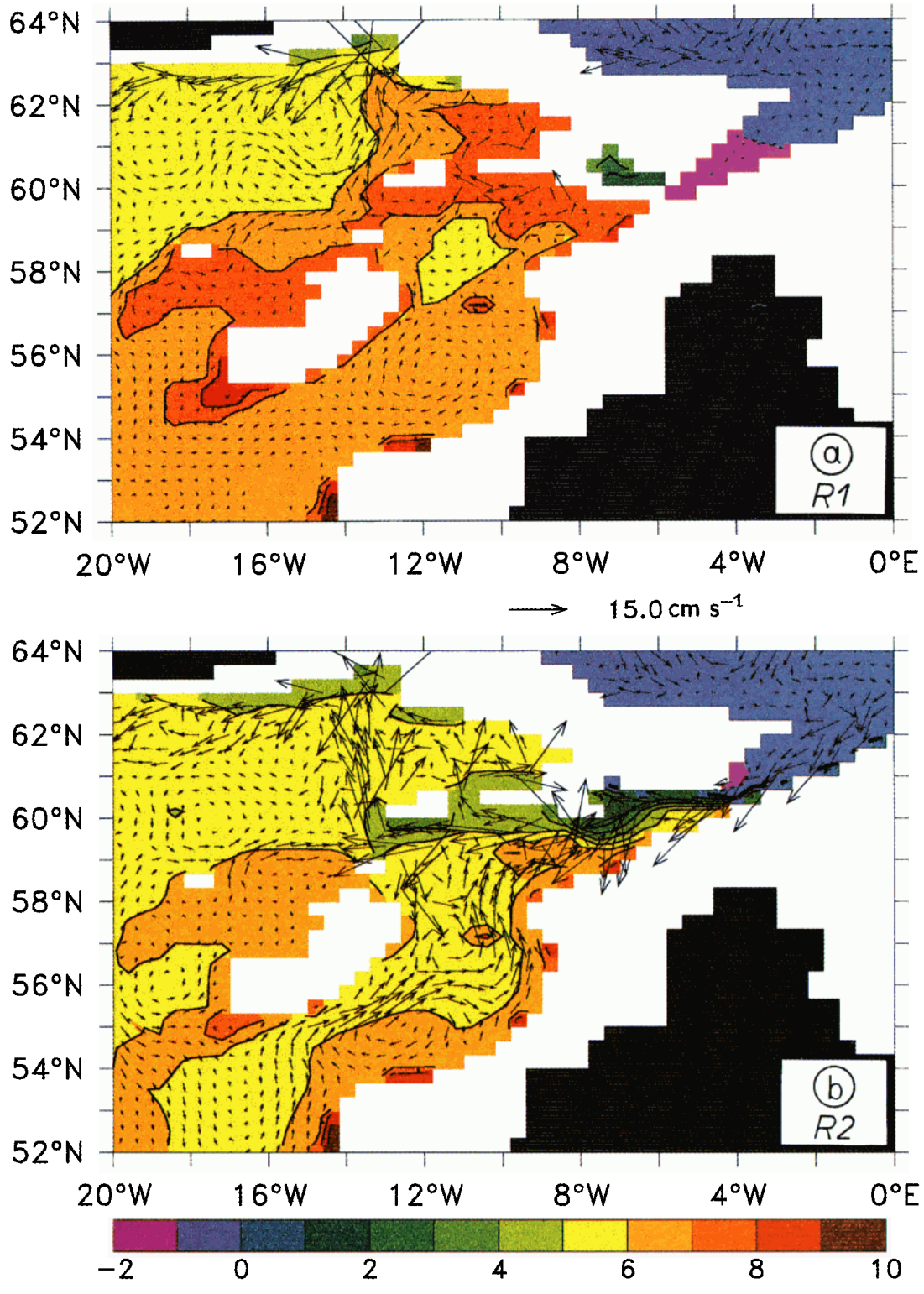

Plate 1. Annual mean potential temperature in degrees Celsius (averaged from 650 to 1750 m) and horizontal velocity in centimeters per second at level 11 (711 m) in the northeast corner of the regional model from (a) R1 and (b) R2, indicating the effect of widening the Faeroe Bank Channel. The contour interval is 1 °C.

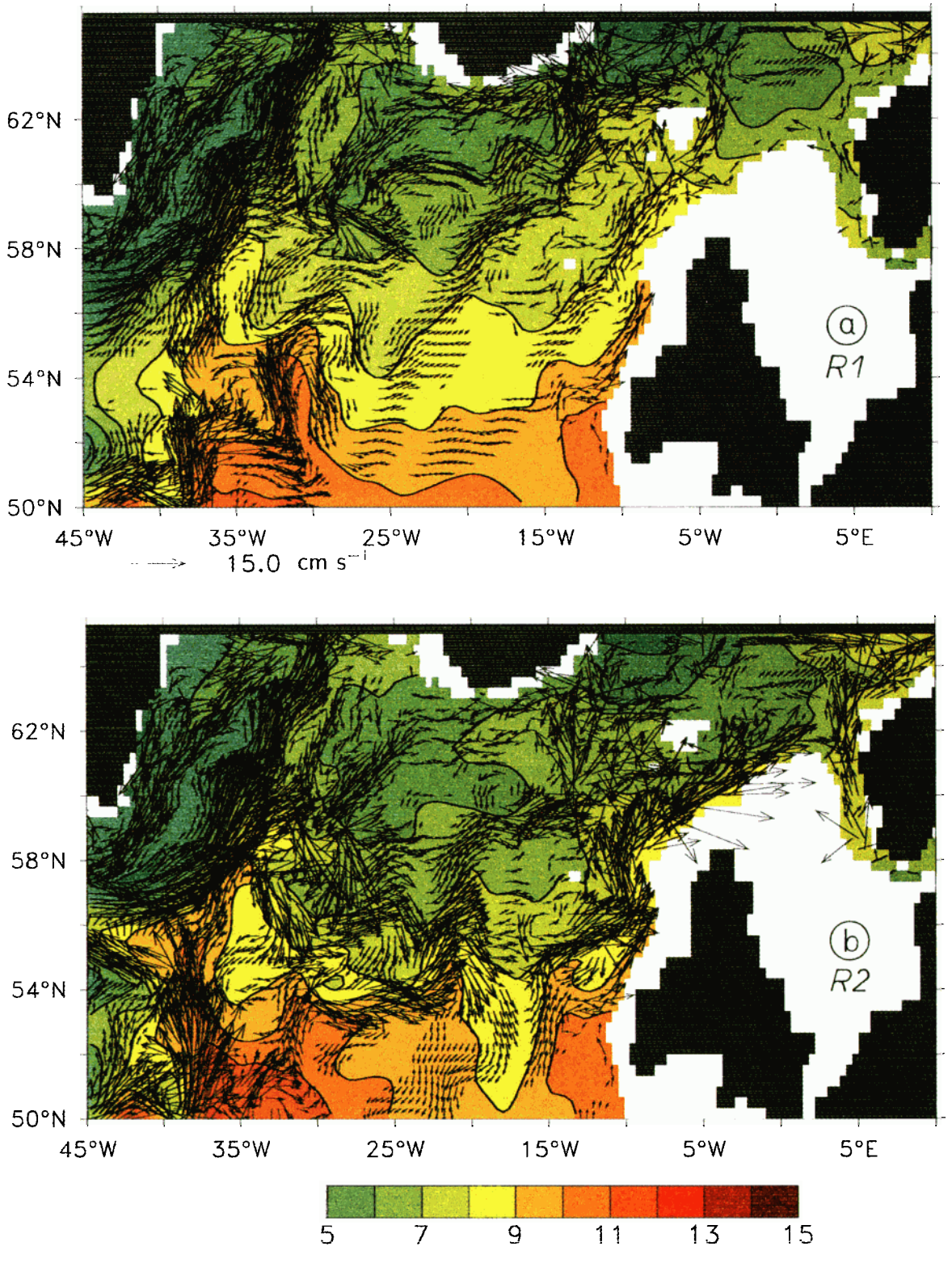

Plate 2. Annual mean potential temperature in degrees Celsius and horizontal velocity in centimeters per second at level 5 (175 m) for experiments (a) R1 and (b) R2, showing the deflection of the NAC due to widening the Faeroe Bank Channel, and for experiments (c) R4 and (d) $R4^{Lev}$. The contour interval is 1 °C.

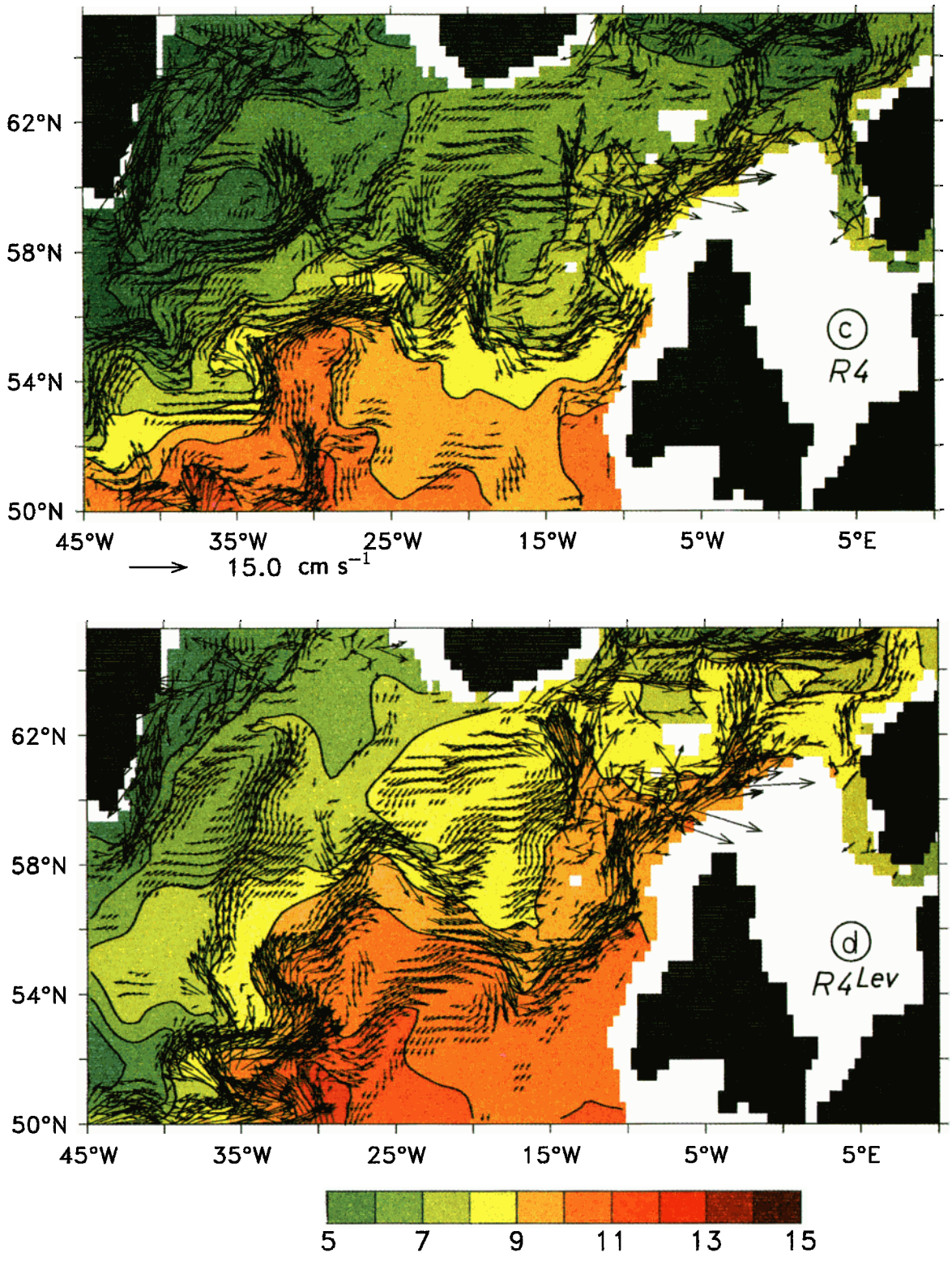

Plate 2. (continued)

experiments; numbers indicate transports between 1000 m and the bottom except in the Faeroe Bank section, where the throughflow occurs at depths above 900 m.

In the reference case R1, deep water production is located mainly in the northern part of the Irminger Basin at the closed boundary and in an area southeast of Iceland [*Ernst*, 1995]. The main sinking areas are indicated by the dotted patches. The source of deep water entering the northeastern Atlantic overflowing the Iceland-Faeroe-Scotland Sills is negligible (Figure 11a). The westward flow of 2 Sv south of Iceland originates from downwelling water south of Iceland. This pattern changes in the experiment R2 with a widened Faeroe Bank Channel (FBC) (Figure 11b). The FBC throughflow now increases to 4.4 Sv. The area of downward transport is shifted to a location at the outlet of the FBC, and 2.3 Sv of this throughflow turn northward to form the DWBC which add up to a westward flow of 3.7 Sv south of Iceland similar to the measurements of *Saunders* [1996], giving 3.2 Sv.

The flow around the Reykjanes Ridge is not significantly different in the experiments shown here. Since a main fraction of the transport is at depths above 2000 m, a crossing of the MAR already occurs north of the Charly-Gibbs Fracture Zone at 52°N for which *Saunders* [1996] reported a deep westward transport of 2.4 Sv. The deep southward flow through the channel is compensated in the upper layer by an enhanced flow of North Atlantic water into the Norwegian Basin. Table 2 shows an increase of the upper layer transport through the 7°W section from 2.5 Sv in the narrow channel cases to 5.1 Sv in R2, suggesting that the bulk of the additional, upper layer flow is confined to the vicinity of the channel.

In the Irminger Basin the deep circulation is mostly affected by the characteristics at the inflow points along the open boundary between Greenland and Iceland. While the DWBC transport near Cape Farewell is similarly weak (10.1 Sv) for experiments R1 and R2 (Figures 11a and 11b) a Denmark Strait inflow of about 10 Sv (Figure 11c) results in an increased transport around Cape Farewell of 17 Sv, similar to the measurements of *Clarke* [1984], that further increases to 19 Sv in the Labrador Sea. The increase in the DWBC off Greenland is associated with an intensification of the northward current along the western flank of the Reykjanes Ridge and hence an intensification of the subpolar gyre in the western basin. This increase is achieved by the restoring to section data at the open boundary and not by the widened FBC.

The changes in the basin-scale structure of the upper layer flow field are illustrated in Plate 2. It shows the emergence in R2 of a concentrated, northeastward flow through Rockall Trough, fed by an eastward flow across the Iceland Basin between roughly 53° and 58°N, branching into two currents near 20°W, west of Rockall Plateau. The southern branch forms an eastern boundary current, flowing through Rockall Trough and continuing northeastward between the Hebridean Shelf and Faeroe Shelf, with typical velocities of 15 – 20 cm/s and a transport of 11.9 Sv in the upper 1000 m at 58°N (9° – 12°W). The northern branch forms a boundary current along the northwestern slope of Rockall Plateau, with velocities not exceeding 5 cm/s and a transport of 3.5 Sv across 58°N (19° – 24°W).

While the current structure and intensity in the Rockall area appear more realistic in case R2, compared, e.g., to the observational picture of *Bersch* [1995], there are still significant deficits in other aspects of the upper layer circulation pattern. As in all the cases with the closed boundary at 65°N, the upper layer water cannot leave the domain in the northeast. Instead the models produce an artificial recirculation with a westward boundary current south of Iceland (Plates 2a and 2b). Its vertically integrated transport at 14°W is 12 Sv in R1 (Figure 10c). In R2 the total westward transport increases to about 16 Sv but is spread over a broader latitudinal range. This model feature is in stark contrast to the observational picture obtained from drifter measurements in the area [*Krauss*, 1995], which indicate an eastward current between 60° and 62°N toward the Iceland-Faeroe Ridge and into the Norwegian Sea.

Another model deficit concerns the main path of the NAC in the vicinity of the MAR. Both R1 (Plate 2a) and R2 (Plate 2b) have the bulk of the NAC flowing north in the Irminger Sea, along the western flank of the MAR. The behavior is similar as in previous CME solutions [*Böning et al.*, 1996] and was interpreted as an effect of the northern boundary formulation in which water is drawn into the Denmark Straits buffer zone to be converted in deep water. The enhanced eastward flow across the Iceland Basin and around Rockall Plateau in R2 is only partly fed by water separating from the main NAC near 51°N, 35°W. The bulk of it originates farther downstream, separating from the NAC north of 58°N. The advection of this colder water leads to a decrease in the temperatures over the Iceland Basin, 56° and 58°N, by about 1°C compared to R1. On the other hand, the stronger northward flow along the eastern boundary in this case increases the upper layer temperature south of Iceland and the Iceland-Faeroe Ridge.

3.5. Combined Effect of Open Boundaries and Widened Channel

In this section the wide channel geometry is tested in conjunction with open boundary conditions at 65°N that permit an overflow of upper layer water between Iceland and Norway (the specified net outgoing transport is 5.6 Sv).

With a free flow across the open boundaries along 65°N (R5) the transport through the FBC is reduced to 2.6 Sv (Figure 11c) which can be attributed to the barotropic outflow between Iceland and Norway. The westward flow of 2.0 Sv south of Iceland now is made up

of FBC throughflow, somewhat low compared to the 3.2 Sv published by *Saunders* [1996]. Table 2 shows that the deep overflow from the Norwegian Sea is reduced to 2.5 and 2.6 Sv in R4 and R5, with only little sensitivity to the different inflow conditions for Θ and S used for the Denmark Strait. On the other hand, the northward flow of upper layer North Atlantic water through the FBC section remains at about 5 Sv, close to the net outflow between Iceland and Norway prescribed at 65°N. The fact that the water transported north over the Rockall-Faeroe area can now leave the model domain northward, results in a significant change in the circulation system south of Iceland. Plate 2c shows that the westward flow south of Iceland obtained in the closed boundary cases is replaced in R4 by an eastward current in the upper layers, more in line with the observational picture.

Comparison with Plate 2b also shows much less northward flow west of the MAR, which is reflected in the disappearance of the suspicious northward tongue of warm water between 35° and 40°W present in R2. Apart from these differences, the flow and temperature patterns are rather similar in the eastern basin, with eastward flow between 55° and 60°N that partly turns south west of Rockall Bank to feed the northward current through Rockall Trough and along the Hebridean Shelf.

The tendency of the model NAC to flow north in the Irminger Basin as seen in the CME and in the regional model versions with small exchange across the Iceland-Scotland Ridge, is in contrast to the flow pattern obtained in some other large-scale circulation models. In the nearly global model of *Semtner and Chervin* [1992], with a northern boundary at 65°N and 1/2° resolution, the NAC crosses the MAR near 50°N in east-northeast direction. It sharply turns westward south of Rockall Plateau and heads to the Denmark Strait, probably for the same reason as in the CME and regional model cases with a closed boundary. A similar more jet-like (and probably unrealistic) continuation of a NAC across the MAR into the northeastern Atlantic is obtained by *Gerdes and Köberle* [1995] with a medium-resolution (1°) North Atlantic model and climatological forcing. *Roberts and Wood* [1997] report a series of four experiments on a 1° × 1° North Atlantic grid, differing in the representation of the ridge topography. Regardless of the varying degree of exchange with the Nordic Seas, the course of the NAC in all cases bears a remarkable similarity with the *Semtner and Chervin* [1992] pattern, that is, eastward continuation along 50°N and retroflection near Rockall. Common to all these models is that the thermal boundary condition at the sea surface contains a restoration, on differing timescales, of the model sea surface temperature to the Levitus climatology.

The possible effect of the thermal forcing condition is examined in experiment $R4^{Lev}$, where the Haney/Han heat flux condition used in R4, i.e., damping to an apparent atmospheric temperature T^* on a timescale varying in space and time, is replaced by a damping of the surface temperature to the monthly mean climatology of *Levitus* [1982], on a timescale of 30 days. Plate 2d shows that the main effect of the different thermal forcing condition in $R4^{Lev}$ concerns only some details of the flow pattern between the MAR and Rockall Bank and a higher surface temperature over much of the eastern basin. The result suggests that the form of the thermohaline surface forcing is of much less importance for the path of the NAC than the numerical representation of the overflow processes.

4. Summary and Discussion

A model of the Subpolar North Atlantic has been used to study the sensitivity of the regional, three-dimensional circulation on different representations of the exchange of water between the Nordic seas and the North Atlantic proper. The basic configuration is identical to that of the CME North Atlantic model with a horizontal resolution of 1/3° × 2/5°, except that the domain is restricted to the latitudinal range 43° to 65°N. A test case showed that the regional model with an open southern boundary reproduces the major aspects of the full CME North Atlantic model in the subpolar area, if the inflow conditions at the southern boundary are taken from the mean CME fields at that latitude and the model is subject to the same northern boundary conditions (i.e., closed wall and damping of Θ and S toward climatology) as the CME. The sensitivity experiments with the regional model can thus contribute to the understanding of the physical processes and model factors affecting the circulation structure and deep water formation in basin-scale models.

The present study has illuminated two main aspects of the circulation in the northeastern North Atlantic: the structure of the upper layer flow, particularly the path of the North Atlantic Current; and the transport of the deep boundary currents and recirculations in the Irminger and Iceland Basins. We will discuss the results in the context of previous studies with large-scale circulation models of medium to high resolution.

The main deep water production areas in the basic CME model with a closed northern boundary were the northern Irminger Basin and the continental slope south of Iceland [*Böning et al.*, 1996; *Ernst*, 1995]. The combined sinking led to a net DWBC transport off Cape Farewell of 10 Sv, in the case of climatological restoring conditions at the northern wall. The regional model runs show that for an artificial widening of the Faeroer Bank Channel which was blocked in the CME, the local downwelling southeast of Iceland is replaced by sinking near the channel entrance. This has only little effect, however, on the DWBC transport in the Iceland Basin and farther downstream. In contrast, the representation of DSOW is of critical importance for the DWBC transport. It increases by 70% if the water mass characteristics of inflowing water are modified toward observed

values (temperatures of 1°C in contrast to climatological values of 3°C). In general, the open boundary results concerning the role of the DSOW inflow conditions on the DWBC transport and the corresponding net export of NADW from the subpolar basin corroborate the results of the closed boundary CME. Open boundaries alone do not alter the subpolar circulation significantly. The main difference is the weakening of the DSOW core characteristics south of the strait in the open boundary case, due to spurious numerical mixing of the overflow water. With respect to the overturning circulation, an opening of the northern boundary (or an explicit simulation of the overflows in models explicitly including the Nordic Seas) may hence result in a weakening of the NADW cell compared to a model with a deep restoring south of the Denmark Strait.

The main importance of simulating the exchange with the Nordic Seas lies in its effect on the structure of the upper layer circulation. The northeastward flow of the NAC across the MAR toward the Rockall Plateau essentially depends on the realization of the water exchange across the Iceland-Scotland Ridge. If the exchange is blocked due to an insufficient lateral resolution of the major deep water pathway, the FBC, there is only a weak flow of upper layer water toward the Rockall-Faeroes region. If at the same time, there is a source of dense deep water in the Denmark Strait area, the bulk of the NAC is drawn north in the Irminger Basin, west of the MAR. A weaker deep water source diminishes the Irminger Current, and a stronger source leads to an intensification of the current; the latter effect is apparent also in the CME experiments of *Döscher et al.* [1994] and *Böning et al.* [1996] and the model study of *Gerdes and Köberle* [1995].

The model realization of a more northeasterly course of the NAC toward Porcupine Bank, Rockall Plateau, and past the Faeroes depends on the relative importance of the deep water sources in the northern Irminger and Iceland Basins, i.e., the efficiency of the respective overflows, and the ability of upper layer, North Atlantic Water to flow out into the Norwegian Sea. A more realistic upper layer circulation than in the CME, with a much weaker Irminger Current and eastward continuation of the NAC, also characterizes the sensitivity experiments of *Roberts and Wood* [1997]. Of major importance in their case seems to be the very weak efficiency of the Denmark Strait overflow that is suggested by the small meridional heat transport: values of 0.4 - 0.7 PW imply a weak meridional overturning and hence a weak NADW production if compared, e.g., to *Döscher et al.* [1994]. Their NAC path, crossing the MAR at about 50°N, is very similar to the standard experiment (weak DSOW forcing and overturning) of *Gerdes and Köberle* [1995]. A similar path was also reported by *Semtner and Chervin* [1992]. While in that model a similar, closed northern boundary as in the CME was used, the NAC looks very different, probably because their 10°-wide restoring zone in the north leads to an additional source of dense water in the northern Iceland Basin, south of the ridge. We obtained a similar effect in a CME test case by including a deep restoration toward Levitus south of the Iceland-Faeroe Ridge.

In summary, the sensitivity experiments presented here have revealed a subtle interplay between the effects of the outflows across the Greenland–Iceland and Iceland–Scotland Ridges: Individually, the former appears as the main control of the transport of the DWBC along the Greenland continental slope and thus of the net meridional overturning circulation in the basin, while the latter has a comparatively small effect on the deep transport in the western basin. However, it is the joint effect of the representation of both overflow regimes that determines the pattern of the upper layer circulation in the northeastern Atlantic.

A realistic representation or parameterization of the effect of these processes in ocean circulation models is of key importance for a realistic simulation of the basin-scale thermohaline circulation, its response to changing atmospheric conditions, and its role in low-frequency climate variations. Toward that goal, work remains to compare and understand the representation in different numerical models of the downslope advection of the dense overflow water south of the Greenland-Scotland Ridge. Model formulations need to be developed that are able to simulate in a more realistic way the effect of the entrainment processes affecting the transport and water mass properties of the overflows in these regions.

Appendix: Open Boundary Conditions

A strict mathematical proof demonstrating that a given open boundary condition (OBC) together with the leading equation forms a well-posed problem is impossible for most practical problems, e.g., a fully three-dimensional set of primitive equations [*Røed and Cooper*, 1987]. Therefore the chosen OBC has to be tested against numerical stability or the ability of free wave propagation out of the model. Experience has shown that a given OBC can perform differently in different geographical locations depending on the local dynamics [*Chapman*, 1985] or when combined with different types of ocean models.

The open boundary conditions used in the present study have been developed and tested by *Stevens* [1990] for use in *Cox* [1984] type primitive equation models like FRAM. The equations used at the open boundaries are discussed in detail by *Stevens* [1990] and *Stevens* [1991]; thus only a brief description will be given here.

Numerous papers have been published dealing with open boundary conditions using a simple linear wave equation

$$\frac{\partial \Phi}{\partial t} = -c_{ph} \frac{\partial \Phi}{\partial n} \tag{A1}$$

for any prognostic variable Φ at the open boundary (e.g., Chapman, 1985). Waves moving toward the boundary with the phase velocity c_{ph} shall propagate

out of the model domain. The local phase speed next to the boundary is computed from the Φ field of the previous timestep before via

$$c_{ph} = -\frac{\partial \Phi^*}{\partial t^*} / \frac{\partial \Phi^*}{\partial n^*} . \quad \text{(A2)}$$

If the flow is directed inward, some prescribed data for the boundary values are used instead, taken either from the interior solutions or from some climatology. Together with the set of equations used for the interior solution this formulation forms a well-posed problem only for free waves. Tests of this type of OBC in combination with the simple one-dimensional shallow water equations show that severe problems occur when bottom friction is added [*Chapman*, 1985].

Another approach is that of *Stevens* [1990]. Instead of using a radiation condition, he simplifies the set of primitive equations to calculate the prognostic values along the boundary. The nonlinear equations of conservation of heat and salt represented here by the variable Φ are reduced to

$$\frac{\partial \Phi}{\partial t} = -c_{ph}\frac{\partial \Phi}{\partial n} - v_n \frac{\partial \Phi}{\partial n} + F^{\Phi} + \gamma(\Phi_{\mathrm{Lev}} - \Phi) , \quad \text{(A3)}$$

where $v_n\, \partial\Phi/\partial n$ represents advection normal to the open boundary, F^{Φ} is the horizontal diffusion term, and $\gamma(\Phi_{\mathrm{Lev}} - \Phi)$ is a restoring term. In order to allow the propagation of internal waves out of the model where advection is directed inward, a correction term $c_{ph}\, \partial\Phi/\partial n$ is added where c_{ph} represents a kind of phase velocity. In the case of zero v_n and diffusion, one is left with the above mentioned radiation condition.

The apparent phase velocity c_{ph} is computed similarly to (2). The advection velocity v_n is derived from the linear equations for conservation of momentum for the internal mode plus an external mode velocity obtained by differentiating the stream function. Both c_{ph} and v_n are limited to allow advection only out of the model and to not exceed the maximum possible velocity given by the CFL criterium. To compute the advection of a tracer, c_{ph} and v_n are set to zero when they are directed inward. In contrast to *Stevens* [1990], our restoration to climatology (inverse timescale of γ of 25 days^{-1}) is switched on only depending on the direction of v_n alone. This greatly enhances the effectiveness, with the number of points where restoring is active being 25% higher than in the procedure of *Stevens* [1990].

The elliptic equation for solving the stream function cannot easily be simplified to obtain a prediction at the open boundary. We follow different approaches for the northern and southern boundary. In contrast to the northern boundary of FRAM, an estimate of Ψ from the Sverdrup relation does not represent a good approximation to the mass transport at 43° or 65°N [*Bryan et al.*, 1995]. For the southern boundary the stream function was defined by mean values of the CME reference solution; for the northern boundary a steady inflow of 5.6 Sv was prescribed between Greenland and Iceland and a corresponding outflow through the Iceland–Norway section.

Acknowledgments. The authors wish to thank Aike Beckmann, Joachim Dengg, Matthew England, and Mark Prater for their helpful comments. We would like to express our thanks to Steve Hankin, NOAA/PMEL, who made available the FERRET plotting package, which we used to visualize the model output, and Annegret Schurbohm for her technical assistance in preparing the figures.

References

Beckmann, A., and R. Döscher, A method for improved representation of dense water spreading over topography in geopotential–coordinate models, *J. Phys. Oceanogr., 27*, 581 - 591, 1997.

Beckmann, A., C. W. Böning, B. Brügge, and D. Stammer, Generation and role of eddy variability in the central North Atlantic Ocean, *J. Geophys. Res., 99*, 20,381–20,391, 1994a.

Beckmann, A., C. W. Böning, C. Köberle, and J. Willebrand, Effects of increased horizontal resolution in a simulation of the North Atlantic Ocean, *J. Phys. Oceanogr., 24*, 326–344, 1994b.

Bennet, A. F., and P. E. Kloeden, The ill–posedness of open ocean models, *J. Phys. Oceanogr., 11*, 1027–1029, 1981.

Bersch, M., On the circulation of the northeastern North Atlantic, *Deep Sea Res., Part I, 42*, 1583–1607, 1995.

Böning, C. W., and R. Budich, Eddy dynamics in a primitive equation model: Sensitivity to horizontal resolution and friction, *J. Phys. Oceanogr., 22*, 361–381, 1992.

Böning, C., F. O. Bryan, W. R. Holland, and R. Döscher, Deep water formation and meridional overturning in a high-resolution model of the North Atlantic, *J. Phys. Oceanogr., 26*, 1142–1164, 1996.

Bryan, K., A numerical investigation of a nonlinear model of a wind-driven ocean, *J. Atmos. Sci., 20*, 594–606, 1969.

Bryan, F. O., and W. R. Holland, A high-resolution simulation of the wind– and thermohaline–driven circulation in the North Atlantic Ocean, in *Parameterization of Small–Scale Processes, Proceedings of the 'Aha Huliko'a Hawaiian Winter Workshop* edited by P. Müller and D. Henderson, pp. 99–115, University of Hawaii, Honolulu, 1989.

Bryan, F. O., C. W. Böning, and W. R. Holland, On the mid-latitude circulation in a high-resolution model of the North Atlantic, *J. Phys. Oceanogr., 25*, 289–305, 1995.

Camp, N. T., and R. L. Elsberry, Oceanic thermal response to strong atmospheric forcing, Part II: The role of one-dimensional processes, *J. Phys. Oceanogr., 8*, 206–214, 1978.

Chapman, D., Numerical treatment of cross-shelf open boundaries in a barotropic coastal ocean model, *J. Phys. Oceanogr., 15*, 1060–1075, 1985.

Chassignet, E. P., L. T. Smith, R. Bleck, and F. O. Bryan, A model intercomparison: Numerical simulations of the North and equatorial Atlantic oceanic circulation in depth and isopycnic coordinates, *J. Phys. Oceanogr., 26*, 1849 - 1867, 1996.

Clarke, A. R., Transport through the Cape Farewell-Flemish Cap section, *Rapp. P.-V. Réun. Cons. Int. Explor. Mer, 185*, 120 - 130, 1984

Cox, M. D., A primitive equation 3–dimensional model of the ocean, *Tech. Rep. 1*, Geophys. Fluid Dyn. Lab., Ocean Group, Princeton Univ., Princeton, N.J., 1984.

Delworth, T., S. Manabe, and R. J. Stouffer, Interdecadal variations of the thermohaline circulation in a coupled ocean–atmoshere model, *J. Clim., 6*, 1993–2011, 1993.

Dickson, R. R., and J. Brown, The prediction of North At-

lantic Deep Water: Sources, rates, and pathways, *J. Geophys. Res., 99*, 12319–12341, 1994.

Döscher, R., and R. Redler, The relative influence of North Atlantic overflow and subpolar deep convection on the thermohaline circulation in an OGCM, *J. Phys. Oceanogr., 27*, in press, 1997

Döscher, R., C. W. Böning, and P. Herrmann, Response of meridional overturning in the North Atlantic to changes in thermohaline forcing in northern latitudes: A model study, *J. Phys. Oceanogr., 24*, 2306–2320, 1994.

England, M. H., Representing the global-scale water masses in ocean general circulation models, *J. Phys. Oceanogr., 23*, 1523–1552, 1993.

Ernst, U., Lagrange'sche Analyse der Bildung und Ausbreitung von Nordatlantischem Tiefenwasser im CME-Modell, M.S. thesis, Inst. für Meereskunde, Kiel, Germany, 1995.

Fine-Resolution Antarctic Model (FRAM) Group, An eddy-resolving model of the southern ocean, *Eos Trans. AGU, 72*, 174–175, 1991.

Gerdes, R., A primitive equation ocean circulation model using a general vertical coordinate transformation, 2, Application to an overflow problem, *J. Geophys. Res., 98*, 14,703–14,726, 1993a.

Gerdes, R., A primitive equation ocean circulation model using a general vertical coordinate transformation, 1, Description and testing of the model, *J. Geophys. Res., 98*, 14,683–14,701, 1993b.

Gerdes, R., and C. Köberle, On the influence of DSOW in a numerical model of the North Atlantic general circulation, *J. Phys. Oceanogr., 25*, 2624–2642, 1995.

Gerdes, R., C. Köberle, and J. Willebrand, The influence of numerical advection schemes on the results of ocean general circulation models, *Clim. Dyn., 5*, 211–226, 1991.

Greatbatch, R. J., A. F. Fanning, A. D. Goulding, and S. Levitus, A diagnosis of interpentadal circulation changes in the North Atlantic Ocean, *J. Geophys. Res., 96*, 22,009–22,023, 1991.

Han, Y.-J., A numerical world ocean general circulation model, Part II: A baroclinic experiment, *Dyn. Atmos. Oceans, 8*, 141–172, 1984.

Haney, R. L., Surface thermal boundary conditions for ocean circulation models, *J. Phys. Oceanogr., 1*, 241–248, 1971.

Holland, W. R., and F. O. Bryan, Sensitivity studies on the role of the ocean in climate change, in: *Ocean Processes in Climate Dynamics: Global and Mediterranean Examples*, NATO ASI Ser. C, Vol 419, edited by P. Malanotte-Rizzoli and A. R. Robinson, pp. 111–134, Kluwer, Dordrecht, 1994.

Isemer, H.-J., and L. Hasse, *The Bunker Climate Atlas of the North Atlantic Ocean, vol. 2, Air-Sea Interactions.* Springer-Verlag, New York, 1987.

Krauss, W., The North Atlantic Current, *J. Geophys. Res., 91*, 5061–5074, 1986.

Krauss, W., Currents and mixing in the Irminger Sea and in the Iceland Basin, *J. Geophys. Res., 100*, 10,851–10,871, 1995.

Levitus, S., Climatological atlas of the world ocean, *NOAA Prof. pap. 13*, U.S. Gov. Print. Off., Washington, D.C., 1982.

Maier-Reimer, E., U. Mikolajewicz, and K. Hasselmann, Mean circulation of the Hamburg LSG OGCM and its sensitivity to the thermohaline forcing, *J. Phys. Oceanogr., 23*, 731–757, 1993.

McCartney, M. S., Recirculating components to the deep boundary current of the northern North Atlantic, *Prog. Oceanogr., 29*, 283–383, 1992.

Meincke, J., Structure and Development of the Greenland-Scotland Ridge, in *The Modern Current Regime Across the Greenland-Scotland Ridge*, edited by M. H. P. Bott, S. Sakov, M. Talwani and J. Thiede, pp. 637 – 650, Plenum, New York, 1983.

National Geophysical Data Center, Digital relief of the surface of the earth, Data Announcement 88-MGG-02, Nat. Oceanic and Atmos. Admin., Boulder, Colo., 1988.

Pacanowski, R., K. Dixon, and A. Rosati, The GFDL modular ocean model users guide, *Technical Report 2*, Geophys. Fluid Dyn. Lab., Ocean Group, Princeton University, Princeton, N.J., 1993.

Price, J., and M. O. Baringer, Outflow and deep water production by marginal seas, *Prog. Oceanogr., 33*, 161–200, 1994.

Roberts, M. J., A. L. New, R. A. Wood, and R. Marsh, An intercomparison of a Bryan–Cox type ocean model and an isopycnic ocean model. Part I.: The subpolar gyre and high–latitude processes, *J. Phys. Oceanogr., 26*, 1465–1527, 1996.

Roberts, M. J., and R. A. Wood, Topographic sensitivity studies with a Bryan–Cox type ocean model, *J. Phys. Oceanogr., 27*, in press, 1997.

Røed, L. P., and C. K. Cooper, A study of various open boundary conditions for wind–forced barotropic numerical ocean models, in *Three–dimensional Models of Marine and Estuarine Dynamics* edited by J. C. J. Nihoul and B. M. Jamart, pp. 305–335, Elsevier, New York, 1987.

Ross, C., Temperature-salinity characteristics of the overflow water in Denmark Strait during "OVERFLOW '73", *Rapp. P. V. Réun. Cons. Int. Explor. Mer, 185*, 111–119, 1984.

Sarmiento, J., On the North and Tropical Atlantic heat balance, *J. Geophys. Res., 91*, 11677–11689, 1986.

Saunders, P. M., Cold outflow from the Faroe Bank Channel, *J. Phys. Oceanogr., 20*, 29–43, 1990.

Saunders, P. M., The flux of overflow water through the Charlie–Gibbs Fracture Zone, *J. Geophys. Res., 99*, 12,343–12,355, 1994.

Saunders, P. M., The flux of dense cold overflow water southeast of Iceland, *J. Phys. Oceanogr., 26*, 85–95, 1996.

Schmitz, W. J., and M. S. McCartney, On the North Atlantic circulation, *Rev. Geophys., 31*, 29–49, 1993.

Schmitz, W. J., On the interbasin–scale thermohaline circulation, *Rev. Geophys., 33*, 151–173, 1995.

Semtner, A. J., and R. M. Chervin, Ocean general circulation from a global eddy–resolving model, *J. Geophys. Res., 97*, 5493–5550, 1992.

Stevens, D. P., On open boundary conditions for three dimensional primitive equation ocean circulation models, *Geophys. Astrophys. Fluid Dyn., 51*, 103–133, 1990.

Stevens, D. P., The open boundary condition in the United Kingdom Fine–Resolution Antarctic Model, *J. Phys. Oceanogr. 21*, 1494–1499, 1991.

Strass, V. H., E. Fahrbach, U. Schauer, and L. Sellmann, Formation of Denmark Strait Overflow Water by mixing in the East Greenland Current, *J. Geophys. Res., 98*, 6907–6919, 1993.

Swift, J. H., The circulation of the Denmark Strait and Iceland-Scotland Overflow Waters in the North Atlantic, *Deep Sea Res., Part A, 31*, 1339–1355, 1984

Weisse, R., U. Mikolajewicz, and E. Maier-Reimer, Decadal variability of the North Atlantic in an ocean general circulation model, *Rep. 108*, 35 pp., Max-Planck Inst. for Meteorol., Hamburg, Germany, 1994.

C. W. Böning and R. Redler, Alfred-Wegener Institut für Polar- und Meeresforschung, Am Handelshafen 12, D-27570 Bremerhaven, Germany (e-mail: rredler@awi-bremerhaven.de).

(Received July 31, 1996; revised November 27, 1996; accepted December 13, 1996.)